NASA TECHNICAL MEMORANDUM

EVALUATION OF A HEMISPHERICAL HEAD FLOW DIRECTION SENSOR FOR INLET DUCT MEASUREMENTS

Donald L. Bennett

Flight Research Center
Edwards, Calif. 93523

1. Report No. TM X-3232	2. Government Accession No.	3. Recipient's Catalog No.		
4. Title and Subtitle EVALUATION OF A HEMISPHERICAL HEAD FLOW DIRECTION SENSOR FOR INLET DUCT MEASUREMENTS		5. Report Date May 1975		
		6. Performing Organization Code		
7. Author(s) Donald L. Bennett		8. Performing Organization Report No. H-862		
9. Performing Organization Name and Address NASA Flight Research Center P. O. Box 273 Edwards, California 93523		10. Work Unit No. 516-51-02		
		11. Contract or Grant No.		
12. Sponsoring Agency Name and Address National Aeronautics and Space Administration Washington, D. C. 20546		13. Type of Report and Period Covered Technical Memorandum		
		14. Sponsoring Agency Code		

15. Supplementary Notes

16. Abstract

A hemispherical head flow direction sensor was tested in a wind tunnel to evaluate its effectiveness for measuring dynamic duct flow direction angles of $\pm 27°$. The tests were conducted at Reynolds numbers of 3.28×10^6 per meter (1.0×10^6 per foot) and 4.92×10^6 per meter (1.5×10^6 per foot) and at Mach numbers from 0.30 to 0.70.

The design criteria for the probe are discussed and the wind tunnel results are presented. Three techniques for deriving flow angles are described.

ORIGINAL PAGE IS
OF POOR QUALITY

17. Key Words (Suggested by Author(s)) Hemispherical head flow direction sensor Duct flow direction Inlet duct measurements Flow direction equations	18. Distribution Statement Unclassified - Unlimited STAR Category 02		
19. Security Classif. (of this report) Unclassified	20. Security Classif. (of this page) Unclassified	21. No. of Pages 22	22. Price* $3.25

EVALUATION OF A HEMISPHERICAL HEAD FLOW DIRECTION SENSOR

FOR INLET DUCT MEASUREMENTS

Donald L. Bennett
Flight Research Center

INTRODUCTION

The primary function of an airplane inlet is to provide the engine with high pressure, uniform airflow. The quantity of the airflow must be varied to match the engine's airflow requirements. High performance, high speed aircraft like the YF-12 airplane resort to bypass systems to meet the flow variance requirement (ref. 1). However, there have been problems with these systems. Opening or closing the bypass doors rapidly has resulted in engine surges or stalls.

For a fuller understanding of the physical phenomena that occur during engine stalls and surges, dynamic flow angularity measurements are desirable in addition to pressure distortion and inlet pressure recovery measurements. To make these measurements in the inlet of the YF-12 aircraft, a fixed hemispherical head flow direction sensor was designed and built at the NASA Flight Research Center. Devices of this type have been extensively investigated (refs. 2 to 5). However, the external configuration of the device designed for the YF-12 airplane was dissimilar to that of most of the sensors investigated because of the close coupling of the transducer assembly and the probe tip. The close coupling was incorporated to improve the accuracy of the dynamic measurements.

This paper describes the sensor and presents and discusses calibration data acquired during wind tunnel tests of the flow direction sensor. The tests were made in the 6- by 6-Foot Wind Tunnel at the NASA Ames Research Center. The tests were made at Mach numbers of 0.30, 0.40, 0.50, 0.60, and 0.70 and at Reynolds numbers of 3.28×10^6 per meter (1.0×10^6 per foot) and 4.92×10^6 per meter (1.5×10^6 per foot). Most of the data presented are for Mach numbers of 0.30, 0.50, and 0.70. Several techniques for determining flow angles are described, and the results of room temperature laboratory frequency response evaluations are presented.

SYMBOLS

Physical quantities in this report are given in the International System of Units (SI) and parenthetically in U.S. Customary Units. The measurements were

made in U.S. Customary Units. Factors relating the two systems are presented in reference 6.

M	Mach number
p	$\left(p_1 + p_2 + p_3 + p_4\right)/4$, kN/m^2 (lb/ft^2)
p_s	free stream static pressure, kN/m^2 (lb/ft^2)
p_t	total pressure, kN/m^2 (lb/ft^2)
p_1, p_2, p_3, p_4, p_5	pressures measured by the hemispherical head flow direction sensor, kN/m^2 (lb/ft^2) (fig. 2)
Δp_α	$p_3 - p_1$, kN/m^2 (lb/ft^2) (fig. 2)
q	free stream dynamic pressure, $0.7M^2 p_s$, kN/m^2 (lb/ft^2)
R	Reynolds number, per m (per ft)
α	true angle of attack (angle between the wind tunnel flow direction and the centerline axis of the probe in the p_1, p_3 plane), deg (fig. 2)
α_c	calculated angle of attack, $0.5 \, \text{arc} \tan \dfrac{p_3 - p_1}{2p_5 - p_3 - p_1}$, deg
α_c'	adjusted angle of attack, $\alpha_c \cos \alpha_c$, deg
β	angle between wind tunnel flow direction and the centerline axis of the probe in the p_2, p_4 plane, deg (fig. 2)
φ	angle between wind tunnel vertical and the p_1, p_3 plane of the probe, deg

The cosines of α, β, and φ are direction cosines, and each is independently determined.

DESIGN CRITERIA

The conditions typically encountered in jet engine ducts were used as design goals for the hemispherical head flow direction sensor. These goals were as follows:

2

Temperature, K (°F)	220 (-65) to 755 (900)
Frequency response, Hz	0 to 100
Flow angularity (α, β), deg	±30
Mach number	0.30 to 0.70
Reynolds number, per m (per ft)	3.28×10^6 (1.0×10^6) to 4.92×10^6 (1.5×10^6)
Total pressure, kN/m^2 (lb/ft^2)	34 (720) to 207 (4320)
Static pressure, kN/m^2 (lb/ft^2)	34 (720) to 103 (2160)

The required temperature range, which is larger than the temperature range encountered under operating conditions, was dictated by safety considerations.

The probe was also designed to provide the minimum aerodynamic interference consistent with the required frequency response. Iberall equations were used as a guide to predict the changes in frequency response that would accompany changes in the size of the ports, the length of the tubing from the ports to the pressure transducers, and the temperature of the system. A combination consistent with the mechanical design considerations was chosen.

SENSOR DESCRIPTION

The hemispherical head flow direction sensor (fig. 1) consisted of a stainless steel housing that contained five pressure transducers. Each transducer was
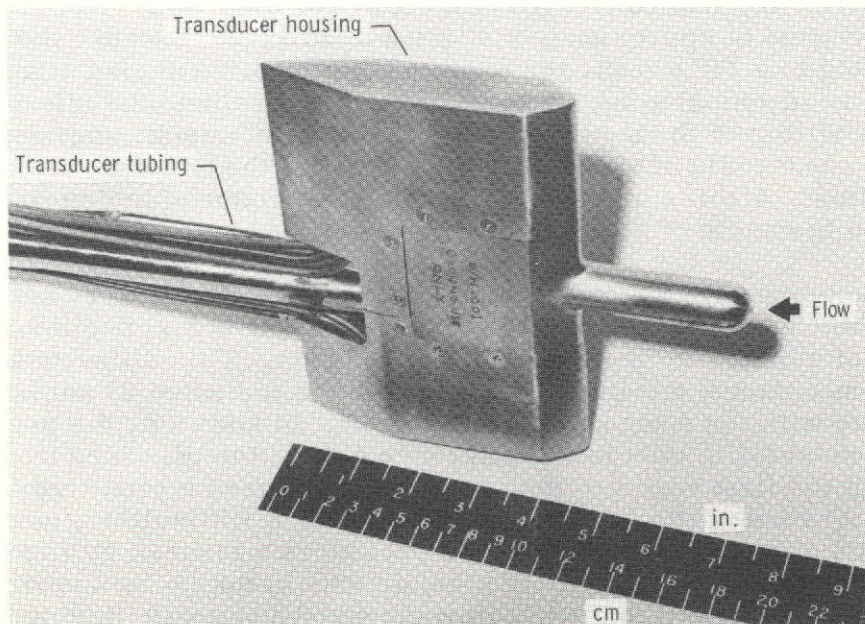
E-24940

Figure 1. Hemispherical head flow direction sensor.

connected to the tip of the probe by tubing approximately 10.2 centimeters (4 inches) long. Tubing of this length was chosen because it permitted adequate frequency response with minimal housing interference. The probe was 1.91 centimeters (0.75 inch) in diameter and contained five ports, each of which was 0.081 centimeter (0.032 inch) in diameter. The inside diameter of the tubing that connected the probe tip port to the pressure transducers was also 0.081 centimeter (0.032 inch). One port, p_5, was on the centerline axis of the hemispherical probe tip (fig. 2). The

other four ports, p_1, p_2, p_3, and p_4, were at an angle of 45° from the centerline axis; p_1 and p_3 were in the vertical plane and used for angle of attack measurements, and p_2 and p_4 were in the horizontal plane and used for angle of sideslip measurements. The sensor housing is a section of the mount that is intended for use in the engine inlet during flight tests.
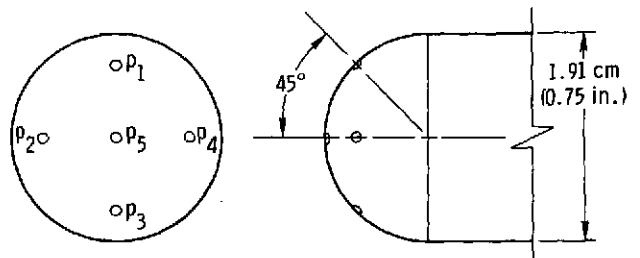

Figure 2. Location of ports in probe tip.

WIND TUNNEL AND LABORATORY TESTS

A wind tunnel calibration was performed on the flow direction sensor at various Mach numbers, angles of attack, angles of sideslip, roll angles, and Reynolds numbers. The Reynolds and Mach numbers investigated were typical of operating conditions in the inlet duct of a YF-12 aircraft. Wind tunnel flow angle was varied by rotating the sensor mechanically with respect to the wind flow. Angle of attack was varied in increments of approximately 4° from 0° to ±27°. Because the wind tunnel sting was limited to a 27° sweep, the positive and negative angles of attack necessitated separate wind tunnel sting configurations. To evaluate the effect of angle of sideslip on the ability of the sensor to measure angle of attack, angle of sideslip was varied during some angle of attack runs by changing the adapters at the end of the wind tunnel sting. A roll angle of 21.5° was also introduced to determine the effect of roll angle on the angle of attack determination.

The data acquired for the computation of angle of sideslip were erroneous. There was a difference of approximately 2° between the actual position of the sensor and the angle of sideslip indicated by the sensor data. This difference was apparently due to a mechanical misalinement, because the indicated 0° angle of sideslip did not coincide with the mechanical setting of 0°. In addition, the pressure line leading from one sideslip port to the reference side of the pressure transducer was pinched during the first series of data runs. This caused a sensitivity change during the calibration of the sensor. Because of these difficulties, no attempt was made to compute angle of sideslip from the pressures measured by the flow direction sensor. The determination of angle of sideslip should not be confused with the changes in angle of sideslip that were introduced mechanically during some angle of attack runs.

During the tests, Reynolds number, Mach number, angle of attack, angle of sideslip, roll angle, free stream dynamic pressure, total pressure, static pressure,

and the pressures measured at the five ports on the probe's hemispherical head were recorded. A tabulation of these data, except for the erroneous p_2 and p_4 data, is given in table 1 for a Reynolds number of 4.92 × 10⁶ per meter (1.5 × 10⁶ per foot). All the data were acquired at room temperature, and no attempt was made to extrapolate the data to higher temperatures.

The data acquired were recorded on paper tape. The raw data were processed and corrected for wind tunnel irregularities by the data processing facility at the Ames Research Center. The data were then placed on magnetic tape and taken to the Flight Research Center, where final computations were made and the data were plotted.

Frequency response evaluations were performed in the laboratory. Figure 3 represents the typical response of the transducing system at room temperature for
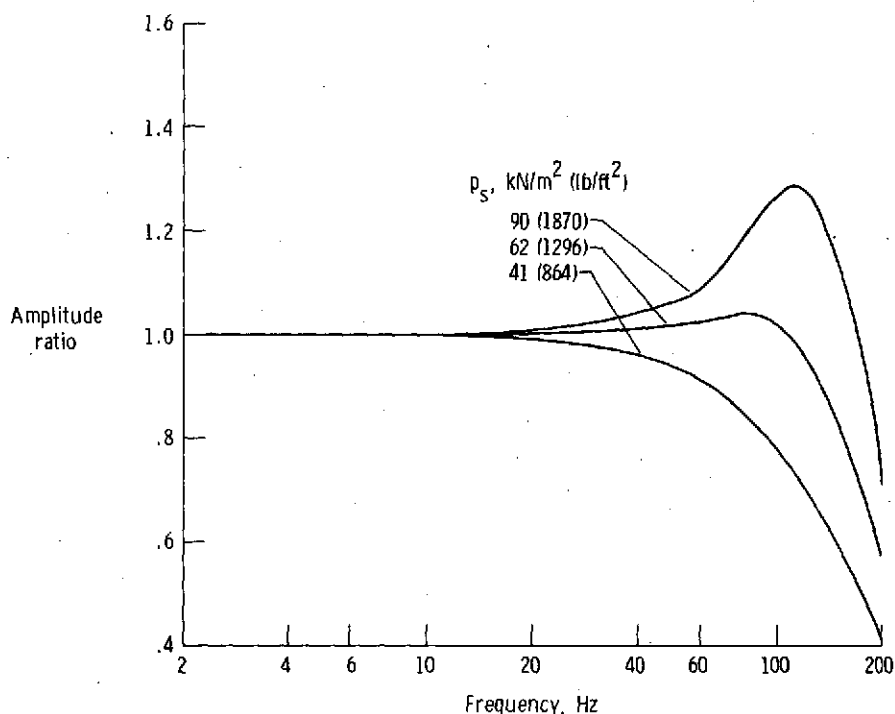
Figure 3. Frequency response of hemispherical head flow direction sensor.

static pressures of 90 kN/m² (1870 lb/ft²), 62 kN/m² (1296 lb/ft²), and 41 kN/m² (864 lb/ft²). The system includes the transducer mounted in the housing and the tubing from the sensor to the probe tip. The frequency response of the system was flat out to 20 hertz. Because of the limitations of the laboratory equipment, the frequency response tests were also conducted at room temperature only.

The predictions obtained from the Iberall equations varied considerably from the results obtained in the laboratory. The reason for this is not known, but the boundary conditions for the equations may have been exceeded.

TABLE 1.—WIND TUNNEL CONDITIONS AND CORRESPONDING SENSOR PRESSURE DATA

[Room temperature; R = 4.92 × 10⁶ per meter (1.5 × 10⁶ per foot)]

(a) Data plotted in figure 4(b).

M	α, deg	β, deg	φ, deg	q, kN/m² (lb/ft²)	p_t, kN/m² (lb/ft²)	p_s, kN/m² (lb/ft²)	p_1, kN/m² (lb/ft²)	p_3, kN/m² (lb/ft²)	p_5, kN/m² (lb/ft²)
.70	-27.47	.44	-.97	9.59 (200.3)	38.83 (811.0)	28.01 (585.0)	37.59 (785.0)	22.46 (469.0)	34.23 (715.0)
.70	-26.48	.42	-.97	9.59 (200.3)	38.83 (811.0)	28.01 (585.0)	37.39 (781.0)	22.89 (478.0)	34.52 (721.0)
.70	-22.50	.36	-.97	9.59 (200.3)	38.83 (811.0)	28.01 (585.0)	36.39 (760.0)	24.04 (502.0)	35.86 (749.0)
.70	-18.46	.30	-.97	9.59 (200.3)	38.83 (811.0)	28.01 (585.0)	35.29 (737.0)	24.90 (520.0)	36.92 (771.0)
.70	-14.40	.24	-.97	9.59 (200.3)	38.83 (811.0)	28.01 (585.0)	34.04 (711.0)	25.18 (526.0)	37.68 (787.0)
.70	-10.38	.17	-.97	9.59 (200.3)	38.83 (811.0)	28.01 (585.0)	32.70 (683.0)	25.90 (541.0)	38.21 (798.0)
.70	-5.34	.09	-.97	9.59 (200.3)	38.83 (811.0)	28.01 (585.0)	30.93 (646.0)	27.29 (570.0)	38.69 (808.0)
.70	-2.84	.05	-.97	9.59 (200.3)	38.83 (811.0)	28.01 (585.0)	30.07 (628.0)	28.11 (587.0)	38.78 (810.0)
.70	-1.35	.02	-.97	9.59 (200.3)	38.83 (811.0)	28.01 (585.0)	29.94 (617.0)	28.49 (595.0)	38.78 (810.0)
.70	-.34	.01	-.97	9.59 (200.3)	38.83 (811.0)	28.01 (585.0)	29.06 (607.0)	28.82 (602.0)	38.73 (809.0)
.70	-1.51	.03	-.97	9.61 (200.8)	39.02 (815.0)	28.20 (589.0)	29.69 (620.0)	28.54 (596.0)	38.93 (813.0)
.70	-.54	.03	-.97	9.61 (200.8)	39.02 (815.0)	28.20 (589.0)	29.49 (616.0)	29.11 (608.0)	39.07 (816.0)
.70	.44	.03	-.97	9.61 (200.8)	39.02 (815.0)	28.20 (·589.0)	29.06 (607.0)	29.11 (608.0)	39.07 (816.0)
.70	1.96	.03	-.97	9.61 (200.8)	39.02 (815.0)	28.20 (589.0)	28.58 (597.0)	29.83 (623.0)	38.93 (813.0)
.70	3.50	.03	-.97	9.61 (200.8)	39.02 (815.0)	28.20 (589.0)	28.06 (586.0)	30.26 (632.0)	39.07 (816.0)
.70	4.55	.03	-.97	9.61 (200.8)	39.02 (815.0)	28.20 (589.0)	27.72 (579.0)	30.60 (639.0)	38.88 (812.0)
.70	9.51	-.16	-.97	9.61 (200.8)	39.02 (815.0)	28.20 (589.0)	26.38 (551.0)	32.41 (677.0)	38.45 (803.0)
.70	13.60	-.22	-.97	9.61 (200.8)	39.02 (815.0)	28.20 (589.0)	25.62 (535.0)	33.85 (707.0)	37.92 (792.0)
.70	17.60	-.29	-.97	9.61 (200.8)	39.02 (815.0)	28.20 (589.0)	25.47 (532.0)	35.14 (734.0)	37.25 (778.0)
.70	21.70	-.35	-.97	9.61 (200.8)	39.02 (815.0)	28.20 (589.0)	24.99 (522.0)	36.48 (762.0)	36.44 (761.0)
.70	25.70	-.41	-.97	9.61 (200.8)	39.02 (815.0)	28.20 (589.0)	23.13 (483.0)	37.39 (781.0)	34.90 (729.0)
.70	-.57	-.41	-.97	9.61 (200.8)	39.02 (815.0)	28.20 (589.0)	29.16 (609.0)	37.39 (781.0)	34.90 (729.0)
.50	-27.68	.44	-.97	7.26 (151.6)	49.17 (1027.0)	41.46 (866.0)	48.22 (1007.0)	37.01 (773.0)	45.53 (951.0)
.50	-26.69	.43	-.97	7.26 (151.6)	49.17 (1027.0)	41.46 (866.0)	48.02 (1003.0)	37.20 (777.0)	45.73 (955.0)
.50	-22.64	.37	-.97	7.26 (151.6)	49.17 (1027.0)	41.46 (866.0)	47.40 (990.0)	37.87 (791.0)	46.78 (977.0)
.50	-18.60	.31	-.97	7.26 (151.6)	49.17 (1027.0)	41.46 (866.0)	46.49 (971.0)	38.02 (794.0)	47.59 (994.0)
.50	-14.53	.24	-.97	7.26 (151.6)	49.17 (1027.0)	41.46 (866.0)	45.58 (952.0)	38.40 (802.0)	48.22 (1007.0)
.50	-10.58	.18	-.97	7.26 (151.6)	49.17 (1027.0)	41.46 (866.0)	44.53 (930.0)	39.21 (819.0)	48.69 (1017.0)
.50	-5.55	.09	-.97	7.26 (151.6)	49.17 (1027.0)	41.46 (866.0)	43.19 (902.0)	40.22 (840.0)	49.08 (1025.0)
.50	-3.05	.05	-.97	7.26 (151.6)	49.17 (1027.0)	41.46 (866.0)	42.47 (887.0)	40.75 (851.0)	49.12 (1026.0)
.50	-1.51	.03	-.97	7.26 (151.6)	49.17 (1027.0)	41.46 (866.0)	42.09 (879.0)	41.18 (860.0)	49.12 (1026.0)
.50	-.49	.01	-.97	7.26 (151.6)	49.17 (1027.0)	41.46 (566.0)	41.80 (873.0)	41.46 (866.0)	49.17 (1027.0)
.50	-1.72	.03	-.97	7.45 (155.6)	49.32 (1030.0)	41.37 (864.0)	41.80 (873.0)	40.94 (855.0)	48.98 (1023.0)
.50	-.75	.01	-.97	7.45 (155.6)	49.32 (1030.0)	41.37 (864.0)	41.56 (868.0)	41.27 (862.0)	48.98 (1023.0)
.50	.26	-.01	-.97	7.45 (155.6)	49.32 (1030.0)	41.37 (864.0)	41.32 (863.0)	41.56 (868.0)	48.93 (1022.0)
.50	1.80	-.03	-.97	7.45 (155.6)	49.32 (1030.0)	41.37 (864.0)	40.84 (853.0)	41.94 (876.0)	48.89 (1021.0)
.50	4.24	-.07	-.97	7.45 (155.6)	49.32 (1030.0)	41.37 (864.0)	40.27 (841.0)	42.61 (890.0)	48.79 (1019.0)
.50	9.38	-.16	-.97	7.45 (155.6)	49.32 (1030.0)	41.37 (864.0)	39.21 (819.0)	44.05 (920.0)	48.50 (1013.0)
.50	17.49	-.29	-.97	7.45 (155.6)	49.32 (1030.0)	41.37 (864.0)	38.16 (797.0)	46.16 (964.0)	47.50 (992.0)
.50	21.43	-.35	-.97	7.45 (155.6)	49.32 (1030.0)	41.37 (864.0)	38.02 (794.0)	46.87 (979.0)	46.73 (976.0)
.50	25.53	-.41	-.97	7.45 (155.6)	49.32 (1030.0)	41.37 (864.0)	37.59 (785.0)	47.44 (995.0)	45.73 (955.0)
.50	13.39	-.22	-.97	7.45 (155.6)	49.32 (1030.0)	41.37 (864.0)	38.45 (803.0)	45.15 (943.0)	48.07 (1004.0)
.50	-.83	.01	-.97	7.45 (155.6)	49.32 (1030.0)	41.37 (864.0)	41.66 (870.0)	41.37 (864.0)	48.84 (1020.0)
.30	-27.74	.45	-.97	4.57 (95.4)	76.56 (1599.0)	71.92 (1502.0)	75.89 (1585.0)	69.04 (1442.0)	74.26 (1551.0)
.30	-26.76	.43	-.97	4.57 (95.4)	76.56 (1599.0)	71.92 (1502.0)	75.79 (1583.0)	69.09 (1443.0)	74.41 (1554.0)
.30	-22.73	.37	-.97	4.57 (95.4)	76.56 (1599.0)	71.92 (1502.0)	75.41 (1575.0)	69.23 (1446.0)	75.08 (1568.0)
.30	-18.71	.31	-.97	4.57 (95.4)	76.56 (1599.0)	71.92 (1502.0)	74.88 (1564.0)	69.43 (1450.0)	75.51 (1577.0)
.30	-10.69	.18	-.97	4.57 (95.4)	76.56 (1599.0)	71.92 (1502.0)	73.74 (1540.0)	70.29 (1468.0)	76.27 (1593.0)
.30	-5.64	.09	-.97	4.57 (95.4)	76.56 (1599.0)	71.92 (1502.0)	72.92 (1523.0)	70.96 (1482.0)	76.51 (1598.0)
.30	-3.10	.05	-.97	4.57 (95.4)	76.56 (1599.0)	71.92 (1502.0)	72.49 (1514.0)	71.34 (1490.0)	76.56 (1599.0)
.30	-1.59	.03	-.97	4.57 (95.4)	76.56 (1599.0)	71.92 (1502.0)	72.25 (1509.0)	71.63 (1496.0)	76.56 (1599.0)
.30	-.61	.01	-.97	4.57 (95.4)	76.56 (1599.0)	71.92 (1502.0)	72.06 (1505.0)	71.77 (1499.0)	76.51 (1598.0)
.30	-1.84	.03	-.97	4.50 (93.9)	76.56 (1599.0)	71.96 (1503.0)	71.92 (1502.0)	71.44 (1492.0)	76.18 (1591.0)
.30	-.81	.01	-.97	4.50 (93.9)	76.56 (1599.0)	71.96 (1503.0)	71.77 (1499.0)	71.58 (1495.0)	76.18 (1591.0)
.30	.19	0.00	-.97	4.50 (93.9)	76.56 (1599.0)	71.96 (1503.0)	71.63 (1496.0)	71.82 (1500.0)	76.18 (1591.0)
.30	1.75	-.03	-.97	4.50 (93.9)	76.56 (1599.0)	71.96 (1503.0)	71.34 (1490.0)	72.06 (1505.0)	76.22 (1592.0)
.30	4.20	-.07	-.97	4.50 (93.9)	76.56 (1599.0)	71.96 (1503.0)	70.96 (1482.0)	72.49 (1514.0)	76.18 (1591.0)
.30	9.25	-.15	-.97	4.50 (93.9)	76.56 (1599.0)	71.96 (1503.0)	70.29 (1468.0)	73.30 (1531.0)	75.99 (1587.0)
.30	13.28	-.22	-.97	4.50 (93.9)	76.56 (1599.0)	71.96 (1503.0)	69.78 (1457.0)	73.97 (1545.0)	75.65 (1580.0)
.30	17.33	-.29	-.97	4.50 (93.9)	76.56 (1599.0)	71.96 (1503.0)	69.43 (1450.0)	74.50 (1556.0)	75.27 (1572.0)
.30	21.33	-.35	-.97	4.50 (93.9)	76.56 (1599.0)	71.96 (1503.0)	69.23 (1446.0)	75.03 (1567.0)	74.79 (1562.0)
.30	25.37	-.41	-.97	4.50 (93.9)	76.56 (1599.0)	71.96 (1503.0)	69.19 (1445.0)	75.46 (1576.0)	74.26 (1551.0)
.30	-.83	.01	-.97	4.50 (93.9)	76.56 (1599.0)	71.96 (1503.0)	71.72 (1498.0)	71.63 (1496.0)	76.18 (1591.0)

TABLE 1.—Continued

(b) Data plotted in figure 5(a).

M	α, deg	β, deg	φ, deg	q, kN/m² (lb/ft²)	P_t', kN/m² (lb/ft²)	P_s', kN/m² (lb/ft²)	P_1', kN/m² (lb/ft²)	P_3', kN/m² (lb/ft²)	P_5', kN/m² (lb/ft²)
.70	-1.59	1.77	-.97	9.51 (198.7)	38.45 (803.0)	27.67 (578.0)	29.16 (609.0)	28.30 (591.0)	38.35 (801.0)
.70	-.62	1.77	-.97	9.51 (198.7)	38.45 (803.0)	27.67 (578.0)	28.92 (604.0)	28.54 (596.0)	38.40 (802.0)
.70	.42	1.77	-.97	9.51 (198.7)	38.45 (803.0)	27.67 (578.0)	28.54 (596.0)	28.87 (603.0)	38.40 (802.0)
.70	1.94	1.77	-.97	9.51 (198.7)	38.45 (803.0)	27.67 (578.0)	28.01 (585.0)	29.49 (616.0)	38.35 (801.0)
.70	4.41	1.77	-.97	9.51 (198.7)	38.45 (803.0)	27.67 (578.0)	27.24 (569.0)	30.36 (634.0)	38.30 (800.0)
.70	9.50	1.77	-.97	9.51 (198.7)	38.45 (803.0)	27.67 (578.0)	26.00 (543.0)	32.18 (672.0)	37.97 (793.0)
.70	13.47	1.77	-.97	9.51 (198.7)	38.45 (803.0)	27.67 (578.0)	25.38 (530.0)	33.52 (700.0)	37.44 (782.0)
.70	17.52	1.77	-.97	9.51 (198.7)	38.45 (803.0)	27.67 (578.0)	25.04 (523.0)	34.71 (725.0)	36.72 (767.0)
.70	21.61	1.77	-.97	9.51 (198.7)	38.45 (803.0)	27.67 (578.0)	24.56 (513.0)	35.91 (750.0)	35.81 (748.0)
.70	25.58	1.77	-.97	9.51 (198.7)	38.45 (803.0)	27.67 (578.0)	22.89 (478.0)	36.92 (771.0)	34.57 (722.0)
.70	-.57	1.29	-.97	9.51 (198.7)	38.45 (803.0)	27.67 (578.0)	28.87 (603.0)	28.63 (598.0)	38.35 (801.0)
.70	-27.64	1.29	-.97	9.51 (198.7)	38.45 (803.0)	27.72 (579.0)	37.11 (775.0)	0.00 (0.0)	33.90 (708.0)
.70	-26.64	1.29	-.97	9.51 (198.7)	38.45 (803.0)	27.72 (579.0)	36.87 (770.0)	22.74 (475.0)	34.28 (716.0)
.70	-22.60	1.29	-.97	9.51 (198.7)	38.45 (803.0)	27.72 (579.0)	35.96 (751.0)	24.13 (504.0)	35.53 (742.0)
.70	-18.61	1.29	-.97	9.51 (198.7)	38.45 (803.0)	27.72 (579.0)	34.86 (728.0)	24.80 (518.0)	36.48 (762.0)
.70	-14.56	1.29	-.97	9.51 (198.7)	38.45 (803.0)	27.72 (579.0)	33.61 (702.0)	25.14 (525.0)	37.25 (778.0)
.70	-10.59	1.29	-.97	9.51 (198.7)	38.45 (803.0)	27.72 (579.0)	32.32 (675.0)	25.76 (538.0)	37.83 (790.0)
.70	-5.59	1.29	-.97	9.51 (198.7)	38.45 (803.0)	27.72 (579.0)	30.60 (639.0)	27.20 (568.0)	38.26 (799.0)
.70	-2.95	1.29	-.97	9.51 (198.7)	38.45 (803.0)	27.72 (579.0)	29.64 (619.0)	28.05 (586.0)	38.35 (801.0)
.70	-1.56	1.29	-.97	9.51 (198.7)	38.45 (803.0)	27.72 (579.0)	29.21 (610.0)	28.49 (595.0)	38.40 (802.0)
.70	-1.53	1.29	-.97	9.51 (198.7)	38.45 (803.0)	27.72 (579.0)	28.87 (603.0)	28.92 (604.0)	38.35 (801.0)
.50	-1.77	1.77	-.97	7.21 (150.5)	48.69 (1017.0)	41.03 (857.0)	41.56 (868.0)	40.84 (853.0)	48.65 (1016.0)
.50	-.74	1.77	-.97	7.21 (150.5)	48.69 (1017.0)	41.03 (857.0)	41.42 (865.0)	41.13 (859.0)	48.65 (1016.0)
.50	.21	1.77	-.97	7.21 (150.5)	48.69 (1017.0)	41.03 (857.0)	41.08 (858.0)	41.32 (863.0)	48.65 (1016.0)
.50	1.82	1.77	-.97	7.21 (150.5)	48.69 (1017.0)	41.03 (857.0)	40.70 (850.0)	41.80 (873.0)	48.65 (1016.0)
.50	4.21	1.77	-.97	7.21 (150.5)	48.69 (1017.0)	41.03 (857.0)	40.65 (849.0)	42.52 (888.0)	48.60 (1015.0)
.50	9.25	1.77	-.97	7.21 (150.5)	48.69 (1017.0)	41.03 (857.0)	39.12 (817.0)	43.86 (916.0)	48.31 (1009.0)
.50	13.39	1.77	-.97	7.21 (150.5)	48.69 (1017.0)	41.03 (857.0)	38.35 (801.0)	44.66 (939.0)	47.83 (999.0)
.50	17.38	1.77	-.97	7.21 (150.5)	48.69 (1017.0)	41.03 (857.0)	38.11 (796.0)	45.92 (959.0)	47.31 (988.0)
.50	21.36	1.77	-.97	7.21 (150.5)	48.69 (1017.0)	41.03 (857.0)	37.87 (791.0)	46.73 (976.0)	46.59 (973.0)
.50	25.48	1.77	-.97	7.21 (150.5)	48.69 (1017.0)	41.03 (857.0)	37.30 (775.0)	47.45 (991.0)	45.68 (954.0)
.50	-.73	1.77	-.97	7.21 (150.5)	48.69 (1017.0)	41.03 (857.0)	41.37 (864.0)	41.22 (861.0)	48.65 (1016.0)
.50	-27.79	1.29	-.97	7.20 (150.4)	48.69 (1017.0)	41.03 (857.0)	47.59 (994.0)	36.82 (769.0)	45.39 (948.0)
.50	-26.80	1.29	-.97	7.20 (150.4)	48.69 (1017.0)	41.03 (857.0)	46.78 (977.0)	37.73 (788.0)	46.44 (970.0)
.50	-22.76	1.29	-.97	7.20 (150.4)	48.69 (1017.0)	41.03 (857.0)	45.96 (960.0)	37.92 (792.0)	47.16 (985.0)
.50	-18.79	1.29	-.97	7.20 (150.4)	48.69 (1017.0)	41.03 (857.0)	45.01 (940.0)	38.30 (800.0)	47.78 (998.0)
.50	-14.73	1.29	-.97	7.20 (150.4)	48.69 (1017.0)	41.03 (857.0)	44.05 (920.0)	39.02 (815.0)	48.26 (1008.0)
.50	-10.75	1.29	-.97	7.20 (150.4)	48.69 (1017.0)	41.03 (857.0)	42.71 (892.0)	40.08 (837.0)	48.65 (1015.0)
.50	-5.75	1.29	-.97	7.20 (150.4)	48.69 (1017.0)	41.03 (857.0)	41.99 (877.0)	40.70 (850.0)	48.65 (1016.0)
.50	-3.15	1.29	-.97	7.20 (150.4)	48.69 (1017.0)	41.03 (857.0)	41.56 (868.0)	41.13 (857.0)	48.65 (1016.0)
.50	-1.72	1.29	-.97	7.20 (150.4)	48.69 (1017.0)	41.03 (857.0)	41.32 (863.0)	41.32 (863.0)	48.69 (1017.0)
.50	-.69	1.29	-.97	7.20 (150.4)	43.69 (1017.0)	41.03 (857.0)	41.32 (863.0)	41.32 (863.0)	48.69 (1017.0)
.30	-1.93	1.78	-.97	4.48 (93.6)	75.84 (1584.0)	71.25 (1488.0)	71.48 (1490.0)	70.96 (1482.0)	75.79 (1583.0)
.30	-.88	1.78	-.97	4.48 (93.6)	75.84 (1584.0)	71.25 (1488.0)	71.34 (1490.0)	71.15 (1486.0)	75.79 (1583.0)
.30	-.15	1.78	-.97	4.48 (93.6)	75.84 (1584.0)	71.25 (1488.0)	71.10 (1485.0)	71.29 (1489.0)	75.75 (1582.0)
.30	1.61	1.78	-.97	4.48 (93.6)	75.84 (1584.0)	71.25 (1488.0)	70.91 (1481.0)	71.53 (1494.0)	75.75 (1582.0)
.30	4.19	1.78	-.97	4.48 (93.6)	75.84 (1584.0)	71.25 (1488.0)	70.53 (1473.0)	72.01 (1504.0)	75.75 (1582.0)
.30	9.19	1.78	-.97	4.48 (93.6)	75.84 (1584.0)	71.25 (1488.0)	69.86 (1459.0)	72.87 (1522.0)	75.27 (1572.0)
.30	13.24	1.78	-.97	4.48 (93.6)	75.84 (1584.0)	71.25 (1488.0)	69.33 (1448.0)	73.50 (1535.0)	75.27 (1572.0)
.30	17.27	1.78	-.97	4.48 (93.6)	75.84 (1584.0)	71.25 (1488.0)	69.04 (1442.0)	74.07 (1547.0)	74.88 (1564.0)
.30	21.27	1.78	-.97	4.48 (93.6)	75.84 (1584.0)	71.25 (1488.0)	68.85 (1438.0)	74.55 (1557.0)	74.41 (1554.0)
.30	25.26	1.78	-.97	4.48 (93.6)	75.84 (1584.0)	71.25 (1488.0)	68.76 (1436.0)	74.98 (1566.0)	73.83 (1542.0)
.30	-.83	1.78	-.97	4.48 (93.6)	75.84 (1584.0)	71.25 (1488.0)	71.34 (1490.0)	71.15 (1486.0)	75.75 (1582.0)
.30	-27.95	1.28	-.97	4.48 (93.6)	75.84 (1584.0)	71.25 (1488.0)	75.08 (1568.0)	68.66 (1434.0)	73.64 (1538.0)
.30	-26.93	1.28	-.97	4.48 (93.6)	75.84 (1584.0)	71.25 (1488.0)	74.98 (1566.0)	68.66 (1434.0)	73.74 (1540.0)
.30	-22.88	1.28	-.97	4.48 (93.6)	75.84 (1584.0)	71.25 (1488.0)	74.60 (1558.0)	68.85 (1438.0)	74.41 (1554.0)
.30	-18.87	1.28	-.97	4.48 (93.6)	75.84 (1584.0)	71.25 (1488.0)	74.07 (1547.0)	69.04 (1442.0)	73.83 (1553.0)
.30	-14.83	1.28	-.97	4.48 (93.6)	75.84 (1584.0)	71.25 (1488.0)	73.54 (1536.0)	69.28 (1447.0)	75.22 (1571.0)
.30	-10.85	1.28	-.97	4.48 (93.6)	75.84 (1584.0)	71.25 (1488.0)	72.92 (1523.0)	69.81 (1458.0)	75.51 (1577.0)
.30	-5.81	1.28	-.97	4.48 (93.6)	75.84 (1584.0)	71.25 (1488.0)	72.16 (1507.0)	70.53 (1473.0)	75.79 (1582.0)
.30	-3.28	1.28	-.97	4.48 (93.6)	75.84 (1584.0)	71.25 (1488.0)	71.72 (1498.0)	70.91 (1481.0)	75.79 (1583.0)
.30	-1.81	1.28	-.97	4.48 (93.6)	75.84 (1584.0)	71.25 (1488.0)	71.48 (1493.0)	71.15 (1485.0)	75.79 (1583.0)
.30	-.77	1.28	-.97	4.48 (93.6)	75.84 (1584.0)	71.25 (1488.0)	***** (*****)	71.34 (1490.0)	75.79 (1583.0)

TABLE 1.—Continued

(c) Data plotted in figure 5(b).

M	α, deg	β, deg	φ, deg	q, kN/m³ (lb/ft²)		p_f, kN/m² (lb/ft²)		p_s, kN/m² (lb/ft²)		p_1, kN/m² (lb/ft²)		p_3, kN/m³ (lb/ft²)		p_5, kN/m² (lb/ft²)	
.70	-27.62	5.07	-.97	9.63	(201.21)	38.88	(812.01)	28.01	(585.01)	37.39	(781.01)	22.36	(467.01)	33.95	(709.01)
.70	-26.50	5.07	-.97	9.63	(201.21)	38.88	(812.01)	28.01	(585.01)	37.11	(775.01)	22.70	(474.01)	34.33	(717.01)
.70	-18.42	5.07	-.97	9.63	(201.21)	38.88	(812.01)	28.01	(585.01)	35.19	(735.01)	0.00	(0.0)	36.63	(765.01)
.70	-14.28	5.07	-.97	9.63	(201.21)	38.88	(812.01)	28.01	(585.01)	33.85	(707.01)	24.28	(507.01)	37.39	(781.01)
.70	-10.32	5.07	-.97	9.63	(201.21)	38.88	(812.01)	28.01	(585.01)	32.51	(679.01)	24.99	(522.01)	37.97	(793.01)
.70	-5.20	5.07	-.97	9.63	(201.21)	38.88	(812.01)	28.01	(585.01)	30.79	(643.01)	27.15	(567.01)	38.45	(803.01)
.70	-2.71	5.07	-.97	9.63	(201.21)	38.88	(812.01)	28.01	(585.01)	29.97	(626.01)	27.96	(584.01)	38.54	(805.01)
.70	-1.26	5.07	-.97	9.63	(201.21)	38.88	(812.01)	28.01	(585.01)	29.49	(616.01)	28.54	(596.01)	38.59	(806.01)
.70	-.01	4.64	-.97	9.63	(201.21)	38.88	(812.01)	28.01	(585.01)	29.02	(605.01)	28.92	(604.01)	38.64	(807.01)
.70	-1.49	4.64	-.97	9.59	(200.21)	38.69	(808.01)	27.87	(582.01)	29.11	(608.01)	28.49	(595.01)	38.59	(806.01)
.70	-.54	4.64	-.97	9.59	(200.21)	38.69	(808.01)	27.87	(582.01)	28.25	(590.01)	28.82	(602.01)	38.54	(805.01)
.70	2.06	4.64	-.97	9.59	(200.21)	38.69	(808.01)	27.87	(582.01)	26.25	(548.01)	29.69	(620.01)	38.59	(806.01)
.70	4.51	4.64	-.97	9.59	(200.21)	38.69	(808.01)	27.87	(582.01)	27.48	(574.01)	30.40	(635.01)	38.50	(804.01)
.70	9.58	4.64	-.97	9.59	(200.21)	38.69	(808.01)	27.87	(582.01)	26.05	(544.01)	32.22	(673.01)	38.16	(797.01)
.70	13.60	4.64	-.97	9.59	(200.21)	38.69	(808.01)	27.87	(582.01)	25.33	(525.01)	33.56	(701.01)	37.63	(786.01)
.70	17.60	4.64	-.97	9.59	(200.21)	38.69	(808.01)	27.87	(582.01)	25.09	(524.01)	34.81	(727.01)	36.92	(771.01)
.70	21.68	4.64	-.97	9.59	(200.21)	38.69	(808.01)	27.87	(582.01)	24.61	(514.01)	35.96	(751.01)	36.01	(752.01)
.70	25.78	4.64	-.97	9.59	(200.21)	38.69	(808.01)	27.87	(582.01)	23.32	(487.01)	36.92	(771.01)	34.75	(726.01)
.70	-.50	4.64	-.97	9.59	(200.21)	38.69	(808.01)	27.87	(582.01)	29.11	(608.01)	28.68	(595.01)	38.59	(806.01)
.50	-27.67	5.09	-.97	7.31	(152.61)	48.98	(1023.01)	41.18	(860.01)	47.74	(997.01)	36.48	(762.01)	45.10	(942.01)
.50	-26.67	5.09	-.97	7.31	(152.61)	48.98	(1023.01)	41.18	(860.01)	47.59	(994.01)	36.68	(766.01)	45.39	(948.01)
.50	-22.64	5.09	-.97	7.31	(152.61)	48.98	(1023.01)	41.18	(860.01)	46.83	(978.01)	36.44	(761.01)	46.20	(965.01)
.50	-18.63	5.09	-.97	7.31	(152.61)	48.98	(1023.01)	41.18	(860.01)	45.96	(960.01)	36.92	(772.01)	47.02	(982.01)
.50	-14.47	5.09	-.97	7.31	(152.61)	48.98	(1023.01)	41.18	(860.01)	45.06	(941.01)	37.78	(789.01)	47.69	(996.01)
.50	-10.43	5.09	-.97	7.31	(152.61)	48.98	(1023.01)	41.18	(860.01)	44.10	(921.01)	38.73	(809.01)	48.22	(1007.01)
.50	-6.50	5.09	-.97	7.31	(152.61)	48.98	(1023.01)	41.18	(860.01)	42.76	(893.01)	39.88	(833.01)	48.55	(1014.01)
.50	-2.88	5.09	-.97	7.31	(152.61)	48.98	(1023.01)	41.22	(861.01)	41.61	(869.01)	40.55	(847.01)	48.65	(1016.01)
.50	-1.36	5.09	-.97	7.23	(151.11)	48.93	(1022.01)	41.22	(861.01)	41.37	(864.01)	41.22	(861.01)	48.69	(1017.01)
.50	-.69	5.09	-.97	7.23	(151.11)	48.93	(1022.01)	41.22	(861.01)	41.90	(875.01)	40.95	(856.01)	48.89	(1021.01)
.50	-.28	4.66	-.97	7.23	(151.11)	48.93	(1022.01)	41.22	(861.01)	41.61	(869.01)	41.22	(861.01)	48.93	(1022.01)
.50	.33	4.66	-.97	7.23	(151.11)	48.93	(1022.01)	41.22	(861.01)	41.37	(864.01)	41.51	(867.01)	48.84	(1020.01)
.50	3.87	4.66	-.97	7.23	(151.11)	48.93	(1022.01)	41.22	(861.01)	41.03	(857.01)	42.61	(890.01)	48.50	(1013.01)
.50	4.31	4.66	-.97	7.23	(151.11)	48.93	(1022.01)	41.22	(861.01)	40.41	(844.01)	43.91	(917.01)	48.07	(1004.01)
.50	-6.50	4.66	-.97	7.23	(151.11)	48.93	(1022.01)	41.22	(861.01)	39.26	(820.01)	45.01	(940.01)	47.54	(993.01)
.50	9.38	4.66	-.97	7.23	(151.11)	48.93	(1022.01)	41.22	(861.01)	38.06	(795.01)	45.92	(959.01)	46.78	(977.01)
.50	13.46	4.66	-.97	7.23	(151.11)	48.93	(1022.01)	41.22	(861.01)	37.92	(792.01)	46.78	(977.01)	45.87	(958.01)
.50	17.40	4.66	-.97	7.23	(151.11)	48.93	(1022.01)	41.22	(861.01)	37.44	(782.01)	47.57	(992.01)	45.87	(958.01)
.50	21.56	4.66	-.97	7.23	(151.11)	48.93	(1022.01)	41.22	(861.01)	41.66	(870.01)	41.22	(861.01)	48.93	(1022.01)
.50	25.63	4.66	-.97	7.23	(151.11)	48.93	(1022.01)	41.22	(861.01)	41.66	(870.01)	41.22	(861.01)	48.93	(1022.01)
.30	-.67	4.66	-.97	7.23	(151.11)	48.93	(1022.01)	41.22	(861.01)	41.66	(870.01)	41.22	(861.01)	48.93	(1022.01)
.30	-27.75	5.11	-.97	4.52	(94.31)	76.22	(1592.01)	71.58	(1495.01)	75.32	(1573.01)	66.09	(1422.01)	73.74	(1540.01)
.30	-26.78	5.11	-.97	4.52	(94.31)	76.22	(1592.01)	71.58	(1495.01)	75.12	(1569.01)	68.04	(1421.01)	73.78	(1541.01)
.30	-22.72	5.11	-.97	4.52	(94.31)	76.22	(1592.01)	71.58	(1495.01)	74.74	(1561.01)	68.23	(1425.01)	74.88	(1564.01)
.30	-18.70	5.11	-.97	4.52	(94.31)	76.22	(1592.01)	71.58	(1495.01)	74.31	(1552.01)	69.09	(1443.01)	75.36	(1574.01)
.30	-14.67	5.11	-.97	4.52	(94.31)	76.22	(1592.01)	71.58	(1495.01)	73.74	(1540.01)	69.67	(1455.01)	75.65	(1580.01)
.30	-10.59	5.11	-.97	4.52	(94.31)	76.22	(1592.01)	71.58	(1495.01)	72.30	(1510.01)	70.38	(1470.01)	75.89	(1585.01)
.30	-5.56	5.11	-.97	4.52	(94.31)	76.22	(1592.01)	71.58	(1495.01)	71.82	(1500.01)	70.81	(1479.01)	75.94	(1586.01)
.30	-2.98	5.11	-.97	4.50	(93.91)	76.18	(1591.01)	71.58	(1495.01)	71.58	(1495.01)	71.05	(1484.01)	75.94	(1586.01)
.30	-1.50	5.11	-.97	4.50	(93.91)	76.18	(1591.01)	71.58	(1495.01)	71.34	(1490.01)	71.25	(1488.01)	76.08	(1589.01)
.30	-.29	4.69	-.97	4.50	(93.91)	76.18	(1591.01)	71.58	(1495.01)	71.29	(1489.01)	71.77	(1499.01)	76.18	(1591.01)
.30	-1.77	4.69	-.97	4.50	(93.91)	76.18	(1591.01)	71.58	(1495.01)	70.86	(1480.01)	72.20	(1508.01)	76.08	(1589.01)
.30	-.77	4.69	-.97	4.50	(93.91)	76.18	(1591.01)	71.58	(1495.01)	70.19	(1466.01)	73.02	(1525.01)	72.25	(1509.01)
.30	.21	4.69	-.97	4.50	(93.91)	76.18	(1591.01)	71.58	(1495.01)	69.71	(1456.01)	73.69	(1539.01)	75.65	(1580.01)
.30	1.71	4.69	-.97	4.50	(93.91)	76.18	(1591.01)	71.58	(1495.01)	59.38	(1444.01)	74.26	(1551.01)	71.82	(1500.01)
.30	4.24	4.69	-.97	4.50	(93.91)	76.18	(1591.01)	71.58	(1495.01)	69.14	(1444.01)	74.74	(1561.01)	74.79	(1562.01)
.30	9.27	4.69	-.97	4.50	(93.91)	76.18	(1591.01)	71.58	(1495.01)	65.00	(1441.01)	75.17	(1570.01)	74.26	(1551.01)
.30	13.30	4.69	-.97	4.50	(93.91)	76.18	(1591.01)	71.58	(1495.01)	71.68	(1497.01)	71.29	(1495.01)	76.12	(1590.01)
.30	17.38	4.69	-.97	4.50	(93.91)	76.18	(1591.01)	71.58	(1495.01)	71.68	(1497.01)	71.29	(1495.01)	76.12	(1590.01)
.30	21.41	4.69	-.97	4.50	(93.91)	76.18	(1591.01)	71.58	(1495.01)	71.68	(1497.01)	71.29	(1495.01)	76.12	(1590.01)
.30	25.48	4.69	-.97	4.50	(93.91)	76.18	(1591.01)	71.58	(1495.01)	71.68	(1497.01)	71.29	(1495.01)	76.12	(1590.01)
.30	-.00	4.69	-.97	4.50	(93.91)	76.18	(1591.01)	71.58	(1495.01)	71.68	(1497.01)	71.29	(1495.01)	76.12	(1590.01)

TABLE 1.—Continued

(d) Data plotted in figure 5(c).

M	α, deg	β, deg	φ, deg	q, kN/m²	(lb/ft²)	p_t, kN/m²	(lb/ft²)	p_s', kN/m²	(lb/ft²)	p_1', kN/m²	(lb/ft²)	p_3', kN/m²	(lb/ft²)	p_5', kN/m²	(lb/ft²)
.70	-28.14	8.75	-.97	9.53	(199.0)	38.78	(810.0)	28.01	(585.0)	37.15	(776.0)	22.22	(464.0)	33.42	(698.0)
.70	-27.16	8.75	-.97	9.53	(199.0)	38.78	(810.0)	28.01	(585.0)	36.92	(771.0)	22.26	(465.0)	33.85	(707.0)
.70	-23.05	8.75	-.97	9.53	(199.0)	38.78	(810.0)	28.01	(585.0)	36.15	(755.0)	23.08	(482.0)	35.10	(733.0)
.70	-19.01	8.75	-.97	9.53	(199.0)	38.78	(810.0)	28.01	(585.0)	35.10	(733.0)	23.32	(487.0)	36.15	(755.0)
.70	-14.95	8.75	-.97	9.53	(199.0)	38.78	(810.0)	28.01	(585.0)	33.85	(707.0)	24.23	(506.0)	36.96	(772.0)
.70	-10.85	8.75	-.97	9.53	(199.0)	38.78	(810.0)	28.01	(585.0)	32.56	(680.0)	25.52	(533.0)	37.54	(784.0)
.70	-5.79	8.75	-.97	9.53	(199.0)	38.78	(810.0)	28.01	(585.0)	30.93	(646.0)	27.15	(567.0)	38.06	(795.0)
.70	-3.17	8.75	-.97	9.53	(199.0)	38.78	(810.0)	28.01	(585.0)	30.00	(626.0)	27.15	(567.0)	38.06	(795.0)
.70	-1.69	8.75	-.97	9.53	(199.0)	38.78	(810.0)	28.01	(585.0)	29.97	(626.0)	28.06	(586.0)	38.21	(798.0)
.70	-.43	8.75	-.97	9.53	(199.0)	38.78	(810.0)	28.01	(585.0)	29.11	(608.0)	29.02	(606.0)	38.40	(802.0)
.70	-2.17	8.75	-.97	9.44	(197.2)	38.54	(805.0)	27.91	(583.0)	29.49	(616.0)	28.15	(588.0)	38.11	(796.0)
.70	-1.19	8.75	-.97	9.44	(197.2)	38.54	(805.0)	27.91	(583.0)	29.87	(610.0)	28.58	(597.0)	38.16	(797.0)
.70	-.14	8.75	-.97	9.44	(197.2)	38.54	(805.0)	27.91	(583.0)	29.45	(615.0)	28.87	(603.0)	38.21	(799.0)
.70	1.50	8.75	-.97	9.44	(197.2)	38.54	(805.0)	27.91	(583.0)	30.26	(632.0)	38.06	(795.0)	38.06	(795.0)
.70	3.96	8.75	-.97	9.44	(197.2)	38.54	(805.0)	27.44	(573.0)	31.98	(668.0)	37.63	(786.0)	37.63	(786.0)
.70	9.09	8.75	-.97	9.44	(197.2)	38.54	(805.0)	25.95	(542.0)	33.42	(698.0)	37.20	(777.0)	37.20	(777.0)
.70	13.06	8.75	-.97	9.44	(197.2)	38.54	(805.0)	25.23	(527.0)	34.62	(723.0)	36.63	(765.0)	36.63	(765.0)
.70	17.09	8.75	-.97	9.44	(197.2)	38.54	(805.0)	24.80	(518.0)	35.62	(723.0)	36.38	(760.0)	38.21	(798.0)
.70	25.23	8.75	-.97	9.44	(197.2)	38.54	(805.0)	22.89	(478.0)	36.87	(770.0)	34.38	(718.0)	38.21	(798.0)
.70	-1.21	8.31	-.97	9.44	(197.2)	38.54	(805.0)	27.91	(583.0)	29.21	(610.0)	28.84	(596.0)	38.06	(795.0)
.50	-28.34	8.76	-.97	7.21	(150.6)	49.12	(1026.0)	41.46	(866.0)	47.74	(997.0)	36.58	(762.0)	45.15	(943.0)
.50	-27.32	8.76	-.97	7.21	(150.6)	49.12	(1026.0)	41.46	(866.0)	47.64	(995.0)	35.58	(764.0)	45.15	(943.0)
.50	-23.25	8.76	-.97	7.21	(150.6)	49.12	(1026.0)	41.46	(866.0)	46.16	(964.0)	36.44	(761.0)	46.11	(963.0)
.50	-19.19	8.76	-.97	7.21	(150.6)	49.12	(1026.0)	41.46	(866.0)	45.28	(945.0)	37.01	(773.0)	46.87	(979.0)
.50	-15.13	8.76	-.97	7.21	(150.6)	49.12	(1026.0)	41.46	(866.0)	45.28	(945.0)	37.87	(791.0)	47.59	(994.0)
.50	-11.02	8.76	-.97	7.21	(150.6)	49.12	(1026.0)	41.46	(866.0)	42.95	(897.0)	40.03	(836.0)	47.59	(994.0)
.50	-5.94	8.76	-.97	7.21	(150.6)	48.69	(1017.0)	41.66	(866.0)	42.23	(882.0)	40.73	(809.0)	48.65	(1005.0)
.50	-3.35	8.76	-.97	7.21	(150.6)	48.69	(1017.0)	41.66	(866.0)	41.66	(872.0)	40.75	(851.0)	48.65	(1016.0)
.50	-1.83	8.76	-.97	7.21	(150.6)	48.69	(1017.0)	41.46	(866.0)	41.13	(859.0)	41.13	(859.0)	48.65	(1016.0)
.50	-.59	8.76	-.97	7.21	(150.6)	48.69	(1017.0)	41.51	(867.0)	41.37	(864.0)	41.37	(864.0)	48.69	(1017.0)
.50	-2.34	8.33	-.97	7.22	(150.7)	48.69	(1017.0)	41.46	(866.0)	41.85	(874.0)	40.70	(850.0)	48.65	(1016.0)
.50	-1.27	8.33	-.97	7.22	(150.7)	48.69	(1017.0)	41.03	(857.0)	42.95	(897.0)	40.03	(836.0)	48.31	(1009.0)
.50	-.33	8.33	-.97	7.22	(150.7)	48.69	(1017.0)	41.03	(857.0)	40.51	(851.0)	40.51	(851.0)	48.31	(1009.0)
.50	1.26	8.33	-.97	7.22	(150.7)	48.69	(1017.0)	41.03	(857.0)	41.08	(858.0)	40.51	(846.0)	48.26	(1008.0)
.50	3.74	8.33	-.97	7.22	(150.7)	48.69	(1017.0)	40.03	(857.0)	42.18	(881.0)	43.43	(907.0)	48.26	(1008.0)
.50	8.85	8.33	-.97	7.22	(150.7)	48.69	(1017.0)	39.78	(836.0)	41.51	(867.0)	44.48	(929.0)	47.45	(991.0)
.50	12.88	8.33	-.97	7.22	(150.7)	48.69	(1017.0)	38.21	(798.0)	44.26	(925.0)	45.44	(949.0)	46.87	(979.0)
.50	16.97	8.33	-.97	7.22	(150.7)	48.69	(1017.0)	37.73	(788.0)	45.44	(949.0)	46.87	(979.0)	46.87	(979.0)
.50	21.02	8.33	-.97	7.22	(150.7)	48.69	(1017.0)	37.02	(773.0)	45.44	(949.0)	46.30	(967.0)	46.11	(964.0)
.50	25.12	8.33	-.97	7.22	(150.7)	48.69	(1017.0)	36.82	(769.0)	47.02	(982.0)	45.25	(945.0)	45.25	(945.0)
.50	-1.30	8.33	-.97	7.22	(150.7)	48.69	(1017.0)	41.03	(857.0)	40.84	(853.0)	40.84	(853.0)	48.31	(1010.0)
.29	-6.05	8.79	-.97	4.29	(89.5)	71.58	(1495.0)	71.15	(1486.0)	70.38	(1470.0)	70.38	(1470.0)	75.70	(1581.0)
.29	-11.13	8.79	-.97	4.29	(89.5)	71.58	(1495.0)	71.15	(1486.0)	70.62	(1475.0)	71.05	(1484.0)	75.75	(1582.0)
.29	-15.18	8.79	-.97	4.29	(89.5)	71.58	(1495.0)	71.15	(1486.0)	71.25	(1488.0)	71.25	(1488.0)	75.75	(1582.0)
.29	-19.26	8.79	-.97	4.29	(89.5)	71.58	(1495.0)	71.15	(1486.0)	71.39	(1491.0)	71.25	(1488.0)	75.70	(1581.0)
.29	-23.34	8.79	-.97	4.29	(89.5)	71.58	(1495.0)	71.15	(1486.0)	71.29	(1489.0)	71.01	(1483.0)	75.55	(1578.0)
.29	-27.27	8.79	-.97	4.29	(89.5)	71.58	(1495.0)	71.15	(1486.0)	71.22	(1488.0)	70.86	(1480.0)	75.51	(1577.0)
.29	-28.42	8.79	-.97	4.29	(89.5)	71.58	(1495.0)	71.15	(1486.0)	70.62	(1480.0)	70.62	(1475.0)	75.48	(1576.0)
.30	25.12	8.79	-.97	4.29	(89.5)	71.58	(1495.0)	71.15	(1486.0)	70.91	(1481.0)	70.91	(1481.0)	76.08	(1589.0)
.30	21.02	8.79	-.97	4.29	(89.5)	71.58	(1495.0)	71.15	(1486.0)	71.05	(1484.0)	71.01	(1483.0)	75.75	(1582.0)
.30	16.97	8.79	-.97	4.29	(89.5)	71.58	(1495.0)	71.15	(1486.0)	71.01	(1484.0)	70.48	(1472.0)	75.70	(1581.0)
.30	12.88	8.79	-.97	4.29	(89.5)	71.58	(1495.0)	71.58	(1495.0)	71.05	(1481.0)	71.05	(1481.0)	75.75	(1582.0)
.30	8.85	8.79	-.97	4.29	(89.5)	71.58	(1495.0)	74.26	(1551.0)	68.56	(1432.0)	74.69	(1560.0)	75.70	(1581.0)
.30	3.74	8.36	-.97	4.48	(93.6)	75.99	(1587.0)	75.22	(1571.0)	73.83	(1542.0)	73.11	(1527.0)	75.75	(1582.0)
.30	1.26	8.36	-.97	4.48	(93.6)	75.99	(1587.0)	75.37	(1569.0)	72.35	(1511.0)	71.05	(1484.0)	75.75	(1582.0)
.30	-.33	8.36	-.97	4.48	(93.6)	75.99	(1587.0)	71.58	(1495.0)	73.11	(1527.0)	70.38	(1470.0)	75.70	(1581.0)
.30	-1.27	8.36	-.97	4.48	(93.6)	75.99	(1587.0)	71.58	(1495.0)	69.62	(1454.0)	71.54	(1494.0)	75.75	(1582.0)
.30	-2.34	8.36	-.97	4.48	(93.6)	75.99	(1587.0)	71.58	(1495.0)	69.86	(1459.0)	71.58	(1495.0)	75.70	(1581.0)
.30	-2.41	8.36	-.97	4.48	(93.6)	75.75	(1582.0)	71.15	(1486.0)	70.62	(1475.0)	70.86	(1480.0)	75.51	(1577.0)
.30	-1.72	8.36	-.97	4.48	(93.6)	75.75	(1582.0)	71.15	(1486.0)	70.86	(1480.0)	71.29	(1489.0)	75.55	(1578.0)
.30	-1.95	8.36	-.97	4.48	(93.6)	75.75	(1582.0)	71.15	(1486.0)	71.05	(1484.0)	71.25	(1490.0)	75.48	(1576.0)
.30	-3.47	8.36	-.97	4.48	(93.6)	75.75	(1582.0)	71.15	(1486.0)	71.92	(1498.0)	71.79	(1498.0)	75.75	(1582.0)
.30	-6.05	8.36	-.97	4.48	(93.6)	75.75	(1582.0)	71.15	(1486.0)	72.35	(1511.0)	70.38	(1470.0)	75.70	(1581.0)
.30	-11.13	8.36	-.97	4.48	(93.6)	75.75	(1582.0)	71.15	(1486.0)	73.11	(1527.0)	69.62	(1454.0)	75.12	(1569.0)
.30	-15.18	8.36	-.97	4.48	(93.6)	75.75	(1582.0)	71.15	(1486.0)	73.83	(1542.0)	68.90	(1432.0)	74.69	(1560.0)
.30	-19.26	8.36	-.97	4.48	(93.6)	75.75	(1582.0)	71.15	(1486.0)	74.26	(1551.0)	68.56	(1425.0)	73.69	(1539.0)
.30	-23.34	8.36	-.97	4.48	(93.6)	75.75	(1582.0)	71.15	(1486.0)	72.13	(1508.0)	68.09	(1422.0)	73.35	(1532.0)
.30	-27.27	8.36	-.97	4.48	(93.6)	75.75	(1582.0)	71.15	(1486.0)	72.25	(1489.0)	68.18	(1424.0)	73.16	(1528.0)
.30	-28.42	8.36	-.97	4.48	(93.6)	75.75	(1582.0)	71.15	(1486.0)	70.62	(1475.0)	74.60	(1558.0)	73.97	(1545.0)
.30	-2.54	8.36	-.97	4.48	(93.6)	75.75	(1582.0)	71.15	(1486.0)	70.67	(1476.0)	75.67	(1476.0)	75.51	(1577.0)

TABLE 1.—Concluded

(e) Data plotted in figure 6.

M	α, deg	β, deg	φ, deg	q, kN/m² (lb/ft²)	p_t, kN/m² (lb/ft²)	p_s, kN/m² (lb/ft²)	p_1, kN/m² (lb/ft²)	p_3, kN/m² (lb/ft²)	p_5, kN/m² (lb/ft²)
.70	.32	.12	21.50	9.65 (201.5)	39.02 (815.0)	28.11 (587.0)	28.97 (605.0)	29.30 (612.0)	38.69 (808.0)
.70	1.27	.49	21.50	9.65 (201.5)	39.02 (815.0)	28.11 (587.0)	28.58 (597.0)	29.45 (615.0)	38.69 (808.0)
.70	2.69	1.04	21.50	9.65 (201.5)	39.02 (815.0)	28.11 (587.0)	28.25 (590.0)	30.07 (628.0)	38.73 (809.0)
.70	4.99	1.92	21.50	9.65 (201.5)	39.02 (815.0)	28.11 (587.0)	27.58 (576.0)	30.88 (645.0)	38.69 (808.0)
.70	9.70	3.73	21.50	9.65 (201.5)	39.02 (815.0)	28.11 (587.0)	26.24 (548.0)	32.56 (680.0)	38.26 (799.0)
.70	13.48	5.16	21.50	9.65 (201.5)	39.02 (815.0)	28.11 (587.0)	25.33 (529.0)	33.66 (703.0)	37.68 (787.0)
.70	17.28	6.57	21.50	9.65 (201.5)	39.02 (815.0)	28.11 (587.0)	24.71 (516.0)	34.81 (727.0)	36.92 (771.0)
.70	21.15	7.98	21.50	9.65 (201.5)	39.02 (815.0)	28.11 (587.0)	24.23 (506.0)	35.96 (751.0)	36.05 (753.0)
.70	24.90	9.30	21.50	9.65 (201.5)	39.02 (815.0)	28.11 (587.0)	23.13 (483.0)	36.72 (767.0)	34.81 (727.0)
.70	25.84	9.62	21.50	9.65 (201.5)	39.02 (815.0)	28.11 (587.0)	22.93 (479.0)	36.72 (767.0)	34.47 (720.0)
.50	.18	.07	21.50	7.22 (150.8)	49.36 (1031.0)	41.70 (871.0)	41.90 (875.0)	41.70 (871.0)	49.12 (1026.0)
.50	1.40	.55	21.50	7.22 (150.8)	49.36 (1031.0)	41.70 (871.0)	41.51 (867.0)	41.99 (877.0)	49.17 (1027.0)
.50	2.87	1.11	21.50	7.22 (150.8)	49.36 (1031.0)	41.70 (871.0)	41.03 (857.0)	42.42 (886.0)	49.17 (1027.0)
.50	5.18	2.01	21.50	7.22 (150.8)	49.36 (1031.0)	41.70 (871.0)	40.65 (849.0)	43.09 (900.0)	49.08 (1025.0)
.50	9.88	3.81	21.50	7.22 (150.8)	49.36 (1031.0)	41.70 (871.0)	39.55 (826.0)	44.34 (926.0)	48.79 (1019.0)
.50	13.64	5.24	21.50	7.22 (150.8)	49.36 (1031.0)	41.70 (871.0)	38.50 (804.0)	45.34 (947.0)	48.36 (1010.0)
.50	17.49	6.67	21.50	7.22 (150.8)	49.36 (1031.0)	41.70 (871.0)	38.06 (795.0)	46.16 (964.0)	47.74 (997.0)
.50	21.27	8.05	21.50	7.22 (150.8)	49.36 (1031.0)	41.70 (871.0)	37.78 (789.0)	46.92 (980.0)	42.90 (896.0)
.50	25.08	9.40	21.50	7.22 (150.8)	49.36 (1031.0)	41.70 (871.0)	37.20 (777.0)	47.50 (992.0)	45.96 (960.0)
.50	24.04	9.72	21.50	7.22 (150.8)	49.36 (1031.0)	41.70 (871.0)	36.87 (770.0)	47.54 (993.0)	45.73 (955.0)
.30	.26	.11	21.50	4.53 (94.6)	76.90 (1606.0)	72.25 (1509.0)	72.20 (1508.0)	72.11 (1506.0)	76.66 (1601.0)
.30	1.47	.58	21.50	4.53 (94.6)	76.90 (1606.0)	72.25 (1509.0)	72.06 (1505.0)	72.35 (1511.0)	76.70 (1602.0)
.30	2.91	1.14	21.50	4.53 (94.6)	76.90 (1606.0)	72.25 (1509.0)	71.77 (1499.0)	72.54 (1515.0)	76.70 (1602.0)
.30	5.23	2.04	21.50	4.53 (94.6)	76.90 (1606.0)	72.25 (1509.0)	71.44 (1492.0)	72.97 (1524.0)	76.61 (1600.0)
.30	9.96	3.87	21.50	4.53 (94.6)	76.90 (1606.0)	72.25 (1509.0)	70.72 (1477.0)	73.74 (1540.0)	76.46 (1597.0)
.30	13.75	5.31	21.50	4.53 (94.6)	76.90 (1606.0)	72.25 (1509.0)	70.19 (1466.0)	74.26 (1551.0)	76.13 (1590.0)
.30	17.53	6.72	21.50	4.53 (94.6)	76.90 (1606.0)	72.25 (1509.0)	69.81 (1458.0)	74.84 (1563.0)	75.79 (1583.0)
.30	21.43	8.14	21.50	4.53 (94.6)	76.90 (1606.0)	72.25 (1509.0)	69.43 (1450.0)	75.27 (1572.0)	75.27 (1572.0)
.30	25.20	9.47	21.50	4.53 (94.6)	76.90 (1606.0)	72.25 (1509.0)	69.28 (1447.0)	75.55 (1578.0)	74.69 (1560.0)
.30	26.14	9.80	21.50	4.53 (94.6)	76.90 (1606.0)	72.25 (1509.0)	69.23 (1446.0)	75.65 (1580.0)	74.50 (1556.0)

INSTRUMENTATION UNCERTAINTIES

The uncertainties of the instrumentation and wind tunnel measurements were estimated as follows:

Measurement	Estimated uncertainty
Wind tunnel flow angularity (α, β, φ), deg	±0.1
Alinement of the sensor centerline axis with the wind tunnel centerline axis (α), deg	±0.3
Mach number	±0.005
Reynolds number, per meter (per foot)	±0.033 × 10⁶ (±0.01 × 10⁶)
Total pressure, N/m² (lb/ft²)	±15 (±0.31)
Static pressure, N/m² (lb/ft²)	±15 (±0.31)
p_1, p_2, p_3, p_4, p_5, N/m² (lb/ft²)	±240 (±5)

METHODS FOR DETERMINING ANGLE OF ATTACK

Three methods for determining angle of attack from the flow direction sensor data were investigated.

Method 1

In the first method, angle of attack was calculated by using the following equation, which is derived in the appendix.

$$\alpha_c = 0.5 \arctan \frac{p_3 - p_1}{2p_5 - p_3 - p_1}$$

The calculated angle of attack was then subtracted from the known angle of attack and plotted as a function of known angle of attack to obtain a correction curve (figs. 4 to 6).
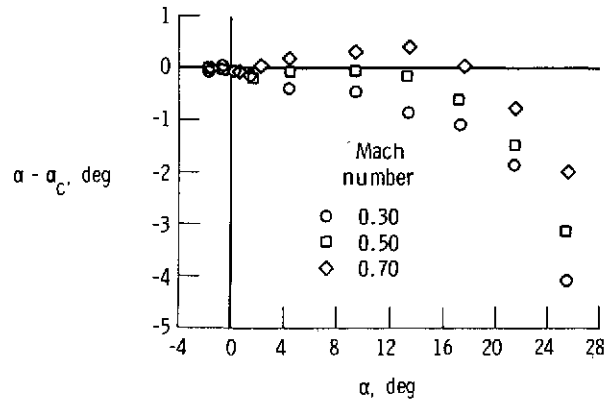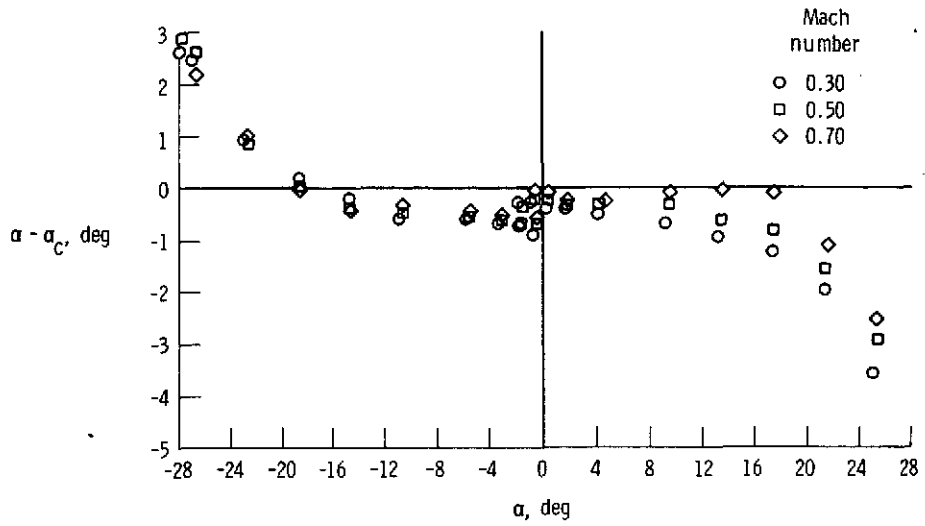
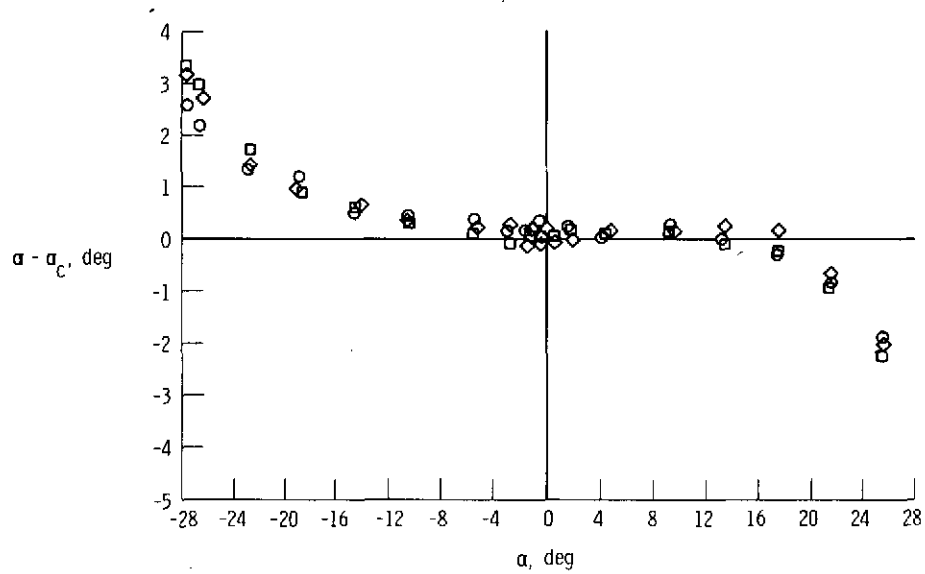(a) $R = 3.28 \times 10^6$ per meter $(1.0 \times 10^6$ per foot).
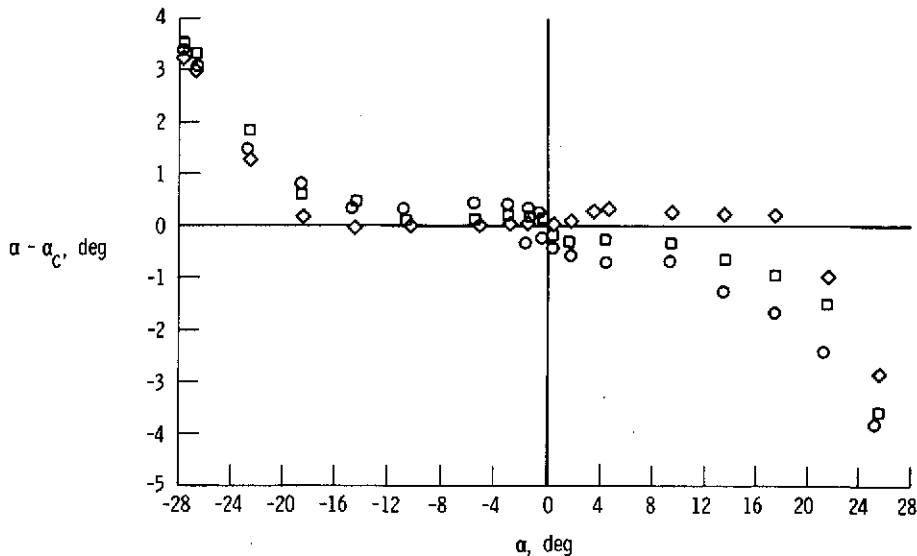
(b) $R = 4.92 \times 10^6$ per meter $(1.5 \times 10^6$ per foot).

Figure 4. Angle of attack correction curves for Reynolds numbers of 3.28×10^6 per meter $(1.0 \times 10^6$ per foot) and 4.92×10^6 per meter $(1.5 \times 10^6$ per foot). $\beta \approx 0°$; $\varphi \approx 0°$.

11

(a) β ≈ 1.5°.

(b) β ≈ 5°.

Figure 5. Angle of attack correction curves for angles of sideslip of approximately 1.5°, 5°, and 8.5°. φ ≈ 0°; R = 4.92 X 10⁶ per meter (1.5 X 10⁶ per foot).
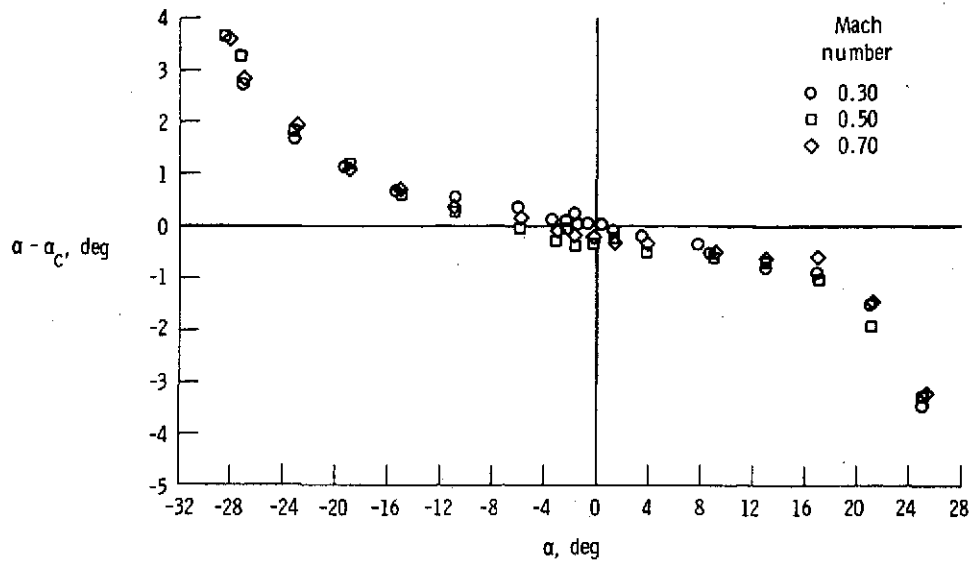
(c) $\beta \approx 8.5°$.

Figure 5. Concluded.
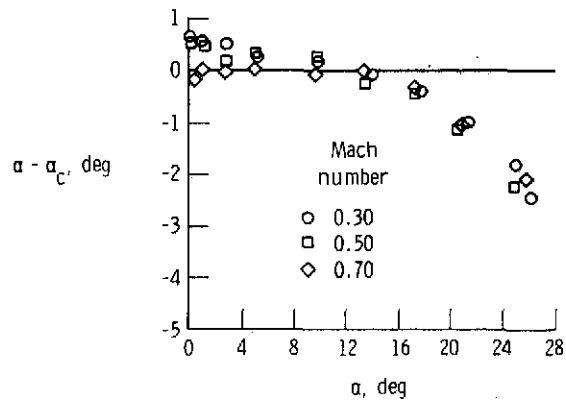
Figure 6. Angle of attack correction curve for a roll angle of 21.5°. $\beta \approx 0°$; $R = 4.92 \times 10^6$ per meter (1.5 × 10⁶ per foot).

Method 2

In the second method, the wind tunnel data were used to obtain a calibration curve. First, Δp_α was calculated for the entire range of angle of attack by using the following equation:

$$\Delta p_\alpha = p_3 - p_1$$

The result was divided by free stream dynamic pressure, q. The resulting values of $\Delta p_\alpha / q$ were plotted as a function of the known angle of attack (fig. 7). After this curve is determined under given environmental conditions, angle of attack can be determined for any value of $\Delta p_\alpha / q$ for equivalent conditions.
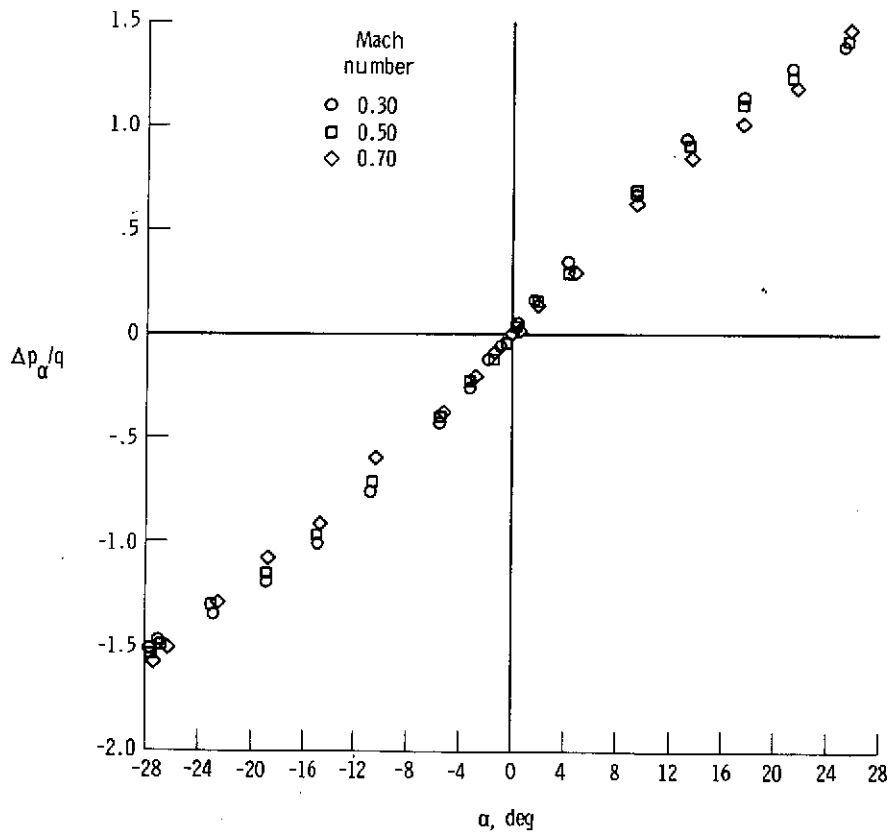
Figure 7. Reference curve derived from method 2. $\beta \approx 0°$; $\varphi \approx 0°$; $R = 4.92 \times 10^6$ per meter (1.5 $\times$ 10^6 per foot).

Method 3

Method 3 is a calibration method similar to method 2. It has the useful property of making accurate determinations of Mach number as well as of angle of attack.

A set of curves of p_5/p versus Mach number is obtained from the wind tunnel data for different angles of attack (fig. 8). Next, a set of curves of $\Delta p_\alpha/p_5$ versus angle of attack is obtained for different Mach numbers (fig. 9). Linear fairings passing through the origin can be made for each Mach number. The value of $(\Delta p_\alpha/p_5)/\alpha$ (the slope) of each of these lines can be plotted versus Mach number (fig. 10).
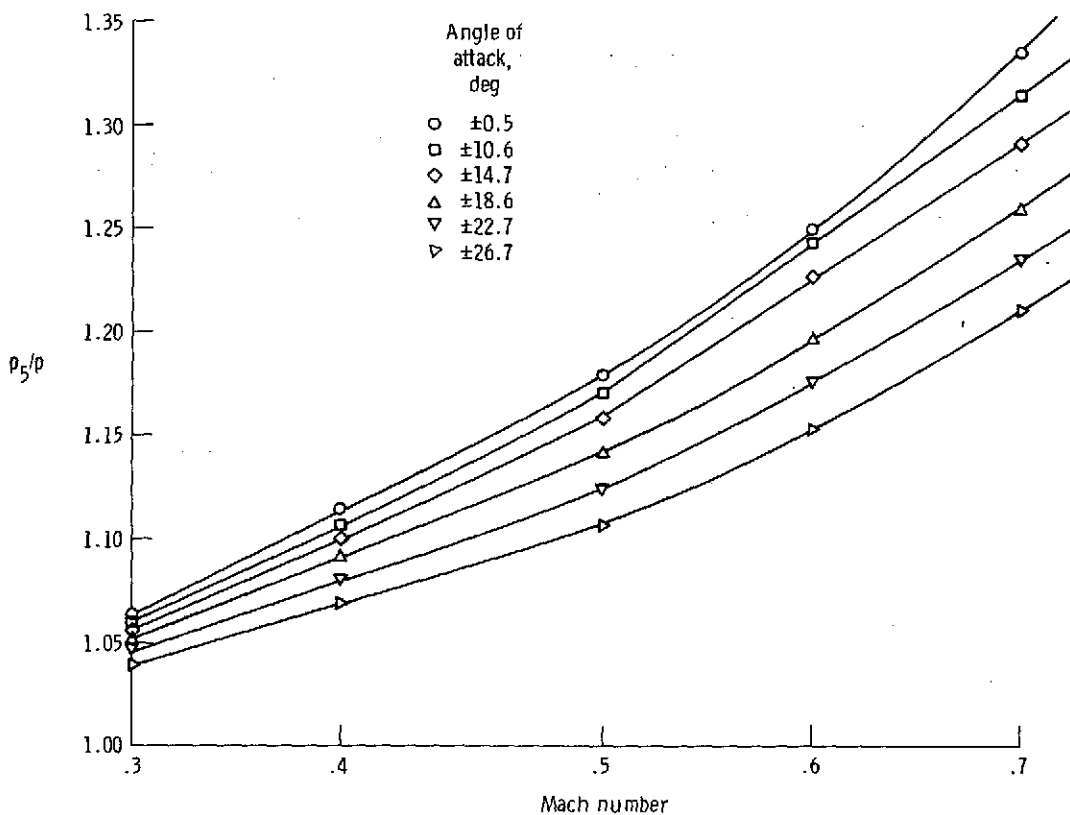
Figure 8. Variation of p_5/p with Mach number and angle of attack. $\beta \approx 0°$; $\varphi \approx 0°$; $R = 4.92 \times 10^6$ per meter $(1.5 \times 10^6$ per foot).
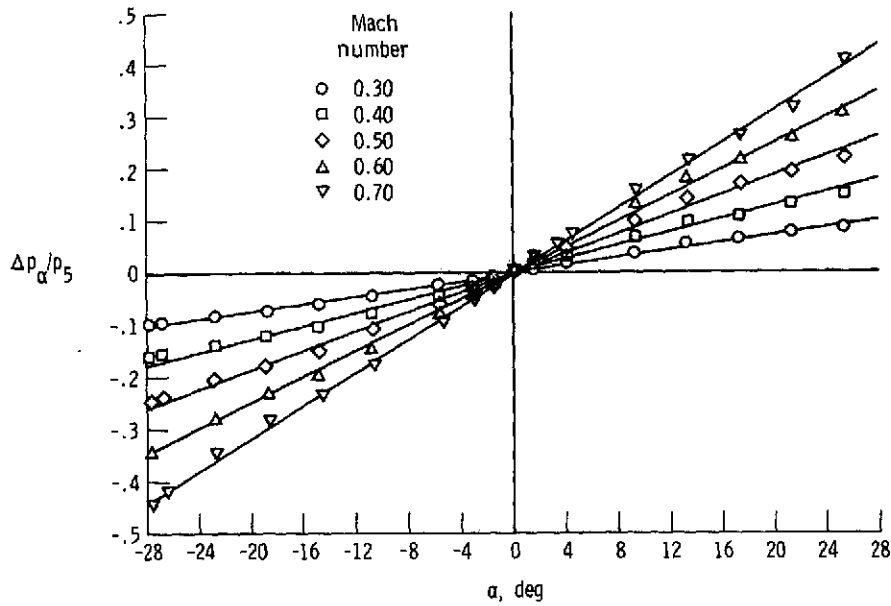
Figure 9. Variation of $\Delta p_\alpha / p_5$ with angle of attack and Mach number. $\beta \approx 0°$; $\varphi \approx 0°$; $R = 4.92 \times 10^6$ per meter $(1.5 \times 10^6$ per foot$)$.
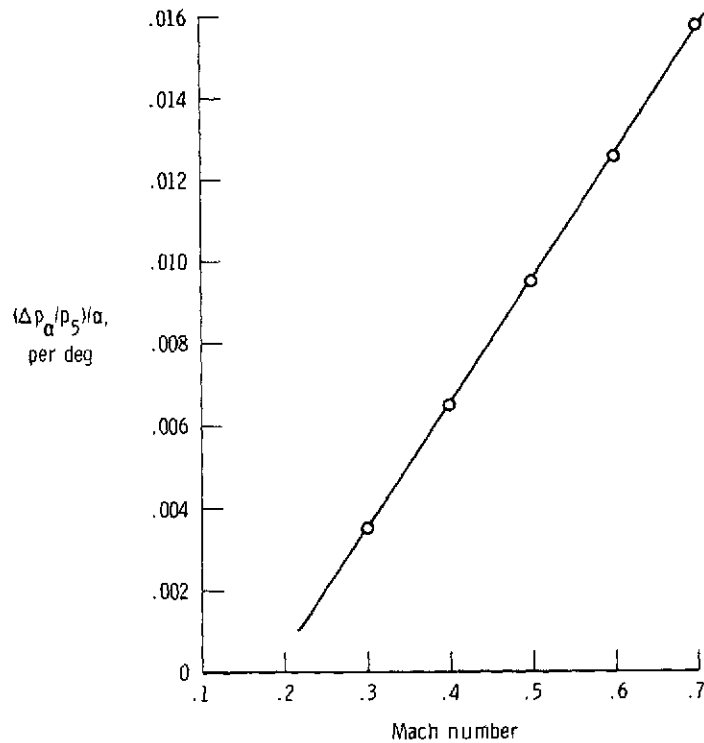

Figure 10. Variation of $(\Delta p_\alpha / p_5)/\alpha$ with Mach number. $\beta \approx 0°$; $\varphi \approx 0°$; $R = 4.92 \times 10^6$ per meter $(1.5 \times 10^6$ per foot$)$.

16

The flow diagram in figure 11 indicates how angle of attack and Mach number can be obtained from these curves. First, an initial angle of attack is assumed and
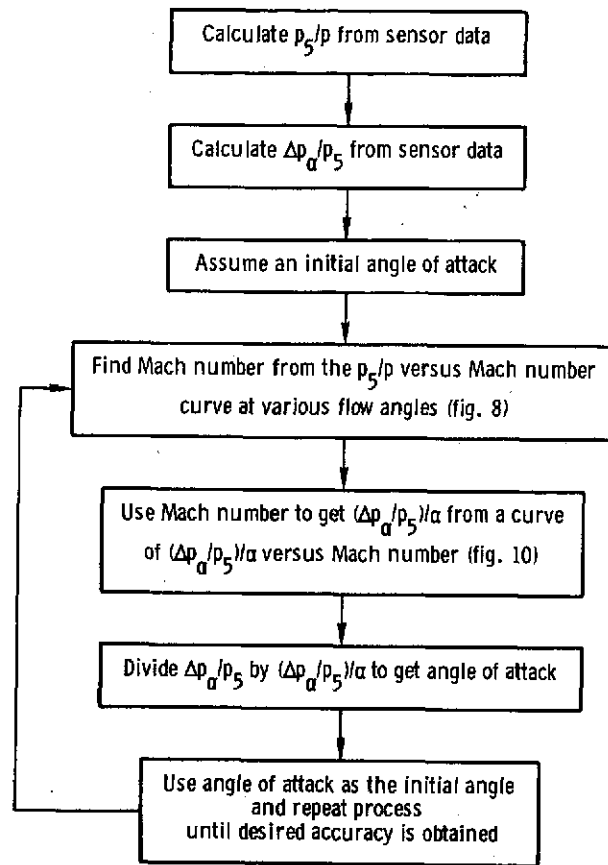
```
┌─────────────────────────────────────┐
│  Calculate p_5/p from sensor data    │
└─────────────────────────────────────┘
                  │
                  ▼
┌─────────────────────────────────────┐
│  Calculate Δp_α/p_5 from sensor data │
└─────────────────────────────────────┘
                  │
                  ▼
┌─────────────────────────────────────┐
│     Assume an initial angle of attack│
└─────────────────────────────────────┘
                  │
                  ▼
┌─────────────────────────────────────────────┐
│  Find Mach number from the p_5/p versus      │
│  Mach number curve at various flow angles    │
│  (fig. 8)                                     │
└─────────────────────────────────────────────┘
                  │
                  ▼
┌─────────────────────────────────────────────┐
│  Use Mach number to get (Δp_α/p_5)/α from a  │
│  curve of (Δp_α/p_5)/α versus Mach number    │
│  (fig. 10)                                    │
└─────────────────────────────────────────────┘
                  │
                  ▼
┌─────────────────────────────────────────────┐
│  Divide Δp_α/p_5 by (Δp_α/p_5)/α to get      │
│  angle of attack                             │
└─────────────────────────────────────────────┘
                  │
                  ▼
┌─────────────────────────────────────────────┐
│  Use angle of attack as the initial angle    │
│  and repeat process                          │
│  until desired accuracy is obtained          │
└─────────────────────────────────────────────┘
```

Figure 11. Procedure for calculating angle of attack and Mach number by using method 3.

an approximate Mach number is found from figure 8. This Mach number is used to find $(\Delta p_\alpha/p_5)/\alpha$ from figure 10, which is a plot of the slopes obtained from figure 9. The value of $\Delta p_\alpha/p_5$ obtained from the sensor data is divided by $(\Delta p_\alpha/p_5)/\alpha$. The result is an approximate angle of attack, which is used to obtain a new Mach number from figure 8. The process is repeated until the difference between two consecutive answers is negligible.

RESULTS AND DISCUSSION

Effects of Flow Angularity and Reynolds Number

The effect of roll angle on the determination of angle of attack can be evaluated by comparing figures 4(b) and 6, which show the angle of attack correction (when

using method 1) for roll angles of 0° and 21.5°, respectively. It can be concluded from this comparison that the effect of roll angles up to 21.5° is negligible.

The effect of angle of sideslip on the determination of angle of attack can be assessed by comparing figures 5(a), 5(b), and 5(c), which show the angle of attack correction (using method 1) for nominal angles of sideslip of 1.5°, 5°, and 8.5°, respectively. This comparison shows that the correction increases slightly with increasing angle of sideslip.

The effect of Reynolds number on the determination of angle of attack is shown by a comparison of figures 4(a) and 4(b), which present the angle of attack correction for Reynolds numbers of 3.28×10^6 per meter (1.0×10^6 per foot) and 4.92×10^6 per meter (1.5×10^6 per foot), respectively. The comparison shows that the effect of Reynolds number on the determination of angle of attack is insignificant over the range tested.

The results of these comparisons simplify the determination of angle of attack from the flow direction sensor measurements regardless of the method used.

Assessment of Methods

The data presented in figures 4 to 6 indicate that the angle of attack calculated by method 1 is within 1° of the known angle of attack up to $\alpha \approx \pm 10°$. Beyond that value, the error increases rapidly to between 3° and 5° at known angles of attack of ±25°.

After studying the data it appeared to be possible to improve the accuracy of the angle of attack measurements by applying a cosine factor to the data. New angles of attack were calculated by using the equation $\alpha'_c = \alpha_c \cos \alpha_c$. Figure 12 is a plot of the data in figure 4(b) with the cosine factor applied. The accuracy of the angle of
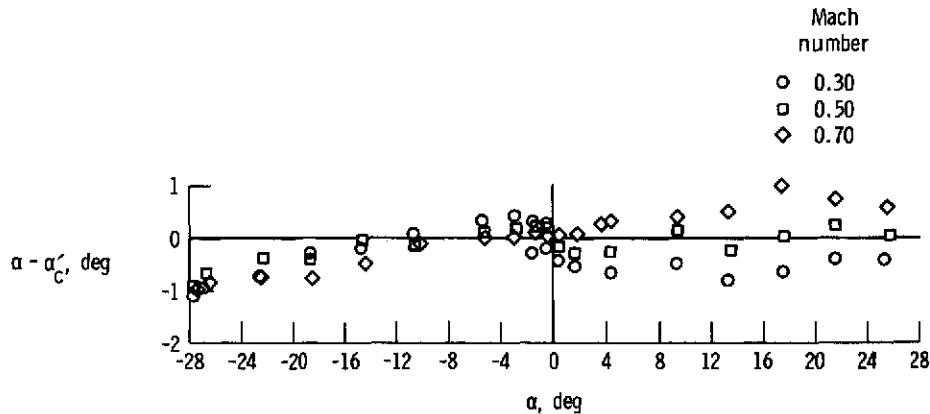
Figure 12. Angle of attack correction curve when cosine factor is applied to data from figure 4(b). $\beta \approx 0°$; $\varphi \approx 0°$; $R = 4.92 \times 10^6$ per meter (1.5×10^6 per foot).

18

attack determination at the higher angles of attack has been improved significantly; the agreement between the calculated and known angles of attack is within 1° throughout the angle of attack range.

In method 2, angle of attack is determined from a reference curve like that in figure 7. The slope $(\Delta p_\alpha/q)/\alpha$ tended to be linear for each Mach number over an angle of attack range of approximately ±8°, but it became increasingly nonlinear as the absolute value of angle of attack increased above 8°. If a best straight line fit to the data is used, the error in angle of attack is less than 1° up to $\alpha \approx \pm20°$. At absolute values greater than 20°, the error increases rapidly.

Since method 3 is a technique of successive approximation, the number of reference curves as well as the number of points in each curve determines the accuracy of the resulting data. Method 3 gives better results at the higher angles of attack because of the relative insensitivity of p_5/p at absolute values of angle of attack up to 10°. This insensitivity is apparent in figure 8.

The results obtained by all three data reduction methods are good, so the choice of method can be based on the type of instrumentation used to support the experiment. All the data required by methods 1 and 3 can be obtained from the flow direction sensor itself. An additional advantage of method 3 is that it has as a byproduct a reasonably accurate determination of local Mach number. However, method 3 also has the disadvantage of requiring many reference curves for the accurate determination of angle of attack.

CONCLUDING REMARKS

A hemispherical head flow direction sensor was tested at room temperature in a wind tunnel at Reynolds numbers of 3.28×10^6 per meter (1.0×10^6 per foot) and 4.92×10^6 per meter (1.5×10^6 per foot) and at Mach numbers from 0.30 to 0.70. Accurate angle of attack measurements were obtained with the sensor.

If the effects of higher temperature on such things as the probe material, pressure transducer sensitivity, and frequency response are taken into account, it should be possible to make adequate high temperature flow direction measurements with the probe.

Flight Research Center
  National Aeronautics and Space Administration
    Edwards, Calif., January 21, 1975

APPENDIX — DERIVATION OF FLOW ANGLE EQUATION

USED IN METHOD 1

The derivation of the flow angle equation used in method 1 begins with the following relationship, which is derived from modified Newtonian flow theory:

$$p_\theta = q(A - B \sin^2 \theta) + p_s \tag{1}$$

where

θ angular displacement from stagnation point

q dynamic pressure, $0.7M^2 p_s$

A,B functions of Mach number

p_θ pressure on a point on a hemispherical body at an angle θ from the stagnation point

p_s free stream static pressure

From equation (1), p_5, p_3, and p_1 (see sketch) can be expressed as:
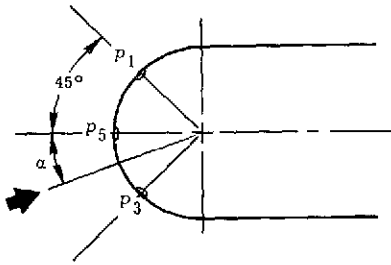
$$p_5 = q(A - B \sin^2 \alpha) + p_s \tag{2}$$

$$p_3 = q[A - B \sin^2 (45 - \alpha)] + p_s \tag{3}$$

$$p_1 = q[A - B \sin^2 (\alpha + 45)] + p_s \tag{4}$$

By applying the identity $\sin^2 \theta = \dfrac{1 - \cos 2\theta}{2}$ to equations (2), (3), and (4), the following equations can be derived:

$$p_5 = q\left[A - \frac{B}{2} (1 - \cos 2\alpha)\right] + p_s \tag{5}$$

$$p_3 = q\left\{A - \frac{B}{2}[1 - \cos (90 - 2\alpha)]\right\} + p_s \tag{6}$$

$$p_1 = q\left\{A - \frac{B}{2} [1 - \cos (2\alpha + 90)]\right\} + p_s \tag{7}$$

Since

$$\cos (C \pm D) = \cos C \cos D \mp \sin C \sin D$$

REFERENCES

1. Burcham, Frank W.; Montoya, Earl J.; and Lutschg, Phillip J.: Description of YF-12C Airplane, Propulsion System, and Instrumentation for Propulsion Research Flight Tests. NASA TM X-3099, 1974.

2. Montoya, Earl J.: Wind-Tunnel Calibration and Requirements for In-Flight Use of Fixed Hemispherical Head Angle-of-Attack and Angle-of-Sideslip Sensors. NASA TN D-6986, 1973.

3. Armistead, Katharine H.; and Webb, Lannie D.: Flight Calibration Tests of a Nose-Boom-Mounted Fixed Hemispherical Flow-Direction Sensor. NASA TN D-7461, 1973.

4. Rogal, B.: Differential Pressure Measurements in Sensing Sideslip and Angle of Attack. Flight Test Instrumentation, Proceedings of the Third International Symposium — 1964, Vol. 3, M. A. Perry, ed., Pergamon Press, 1965, pp. 1-22.

5. Hutton, P. G.: Static Response of a Hemispherical-Headed Yawmeter at High Subsonic and Transonic Speeds. C.P. No. 401, British A.R.C., 1958.

6. Mechtly, E. A.: The International System of Units — Physical Constants and Conversion Factors. Second Revision. NASA SP-7012, 1973.

the angles inside the brackets in equations (6) and (7) can be written

$$\cos (90 - 2\alpha) = \sin 2\alpha \tag{8}$$

$$\cos (2\alpha + 90) = -\sin 2\alpha \tag{9}$$

By making these substitutions,

$$p_3 = q\left[A - \frac{B}{2}(1 - \sin 2\alpha)\right] + p_s \tag{10}$$

$$p_1 = q\left[A - \frac{B}{2}(1 + \sin 2\alpha)\right] + p_s \tag{11}$$

Then the following transformation can be made:

$$p_3 - p_1 = x \tag{12}$$

$$p_5 - p_1 = y \tag{13}$$

From equations (5), (10), and (11),

$$x = qB \sin 2\alpha \tag{14}$$

$$y = \frac{qB}{2}(\cos 2\alpha + \sin 2\alpha) \tag{15}$$

and

$$\frac{y}{x} = \frac{\cos 2\alpha + \sin 2\alpha}{2 \sin 2\alpha} = \frac{1 + \cot 2\alpha}{2} \tag{16}$$

from which the following equation is obtained:

$$\cot 2\alpha = \frac{2y}{x} - 1 \tag{17}$$

Then, from equation (17),

$$\tan 2\alpha = \frac{x}{2y - x} \tag{18}$$

Therefore

$$\alpha = 0.5 \tan^{-1}\left(\frac{x}{2y - x}\right) \tag{19}$$

By substituting from equations (12) and (13), the final flow angle equation is derived:

$$\alpha = 0.5 \tan^{-1}\left(\frac{p_3 - p_1}{2p_5 - p_3 - p_1}\right) \tag{20}$$